INTERNATIONAL UNIVERSITY LIAISON INDONESIA

BACHELOR'S THESIS

PARAMETRIC ANALYSIS ON WING STRUCTURAL COMPONENT OF AN AERIAL FIREFIGHTING AIRCRAFT (BARUNA-1)

By

Kinesha Rahma Kinanti
11201901020

Presented to the Faculty of Engineering
In Partial Fulfilment Of the Requirements for the Degree of

SARJANA TEKNIK
In
AVIATION ENGINEERING

FACULTY OF ENGINEERING

BSD City 15345
Indonesia
February 2023

APPROVAL PAGE

PARAMETRIC ANALYSIS ON WING STRUCTURAL COMPONENT OF AN AERIAL FIREFIGHTING AIRCRAFT (BARUNA-1)

KINESHA RAHMA KINANTI
11201901020
Presented to the Faculty of Engineering
In Partial Fulfillment of the Requirements for the Degree of

SARJANA TEKNIK
In
AVIATION ENGINEERING

FACULTY OF ENGINEERING

Dr. Eng. Ressa Octavianty	________
Thesis Advisor	Date
Triwanto Simanjuntak, PhD	________
Thesis Co-Advisor	Date
Dipl.-Ing. Sentot Wahjoe Goeritno M.Si.	________
Dean of Faculty of Engineering	Date

EXAMINERS APPROVAL PAGE

Dr. Ir. Erie Sandhita
Examiner 1

Date

Ir. Setyo U. Soekarsono, M.Sc., M.M.
Examiner 2

Date

STATEMENT BY THE AUTHOR

I hereby declare that this submission is my own work and to the best of my knowledge, it contains no material previously published or written by another person, nor material which to a substantial extent has been accepted for the award of any other degree or diploma at any educational institution, except where due acknowledgement is made in the thesis.

Kinesha Rahma Kinanti	
Student	Date

ABSTRACT

Parametric Analysis on Wing Structural Component of An Aerial Firefighting Aircraft (Baruna-1)

by

Kinesha Rahma Kinanti

Dr. Eng. Ressa Octavianty, Advisor

Triwanto Simanjuntak, PhD, Co-Advisor

This study analyzed the wing structural components of an aerial firefighting aircraft, namely the Baruna-1. This aircraft is a conventional subsonic aircraft designed by the IULI design team (Inferno) as part of the 2022 AIAA design competition. From the conceptual design and its preliminary analysis, this aircraft has a maximum take-off mass (MTOM) of $\sim$ 144 560 kg (318 754.8 lb) and has met all the requirements set by the FAA 14 CFR Part 25. Nevertheless, the dimension of the wing structural components, such as rib, spar, and skin, were uniform along the span, taken from benchmark studies and references. Considering the aircraft load subjected to the wing structure, those wing components were examined to ensure the aircraft's safety. The structural data constructed using CAD software (OnShape) and the aerodynamic loads from OpenVSP were used to calculate the dimension of rib, spar, and skin by implementing lightweight structure analysis. The analysis was made under static load for the wing with a clean configuration at zero angles of incidence. The result showed that rib, spar, and skin vary along the span in order to be able to sustain the wing load; that is 94.29% difference between the skin thickness on the tip and root, 91.47% between front and aft spar thickness, and 93.8% for rib thickness on the tip and the root.

Keyword: *Aircraft Structure, Wing Structural Analysis, Wing Loading, Wing Skin Thickness, Rib Thickness, Spar Thickness*

ACKNOWLEDGEMENTS

Firstly, I would like to express my deepest gratitude to my advisors, Dr. Eng. Ressa Octavianty and Triwanto Simanjuntak, PhD, whose vast wisdom and wealth of experience have inspired me throughout my studies. Secondly, I would like to express my deepest gratitude to my senior, Teddy Matthew Sunandar, who has given me guidance throughout the process of my research. The completion of this research would not have been possible without their generosity in providing me knowledge and expertise. I would also like to express my sincere gratitude for the support that my family, especially my father, has given to me. Their belief in me has kept my spirit and motivation high throughout my research process. In addition, I would be remiss if I did not mention how grateful I am to have Rafiandra Dayansya, LT.SBLS, the Inferno Team, and all of my friends for helping and supporting me ever since the beginning.

Contents

List of Figures

List of Tables

List of Abbreviations

AIAA	**A**merican **I**nstitute of **A**eronautics and **A**stronautics
AR	**A**spect **R**atio
CAD	**C**omputer **A**ided **D**esign
FAR	**F**ederal **A**viation **R**egulations
MAC	**M**ean **A**erodynamic **C**hord
MGC	**M**ean **G**eometric **C**hord
MTOW	**M**aximum **T**ake **O**ff **W**eight
SAAS	**S**oftware **A**s **A** **S**ervice

Dedicated to my parents

CHAPTER 1
INTRODUCTION

1.1 Problem Statement

As a participation of the AIAA Aircraft Design Competition 2021-2022, Inferno team has designed an aerial firefighting aircraft, namely Baruna-1 (see Fig 1.1), a large widebody conventional type of aircraft with 4500 km of maximum mission range with full payload and 12 500 km (6749.5 nm) ferry range under full fuel capacity. With maximum take-off mass, MTOM $\sim$ 144 560 kg (318 754.8 lbm), the aircraft is designed to use four Europrop TP400-D6 for the engines resulting in 44 260 hp of total power. With a total capacity of 8000 gallons of fire retardant, Baruna-1 uses two water pumps with a retardant reload of 1761 gal/min and a vacuum pump with a retardant reload of $\sim$ 920 gal/min for the ground support. Detail information and design process, including performance and stability analysis to comply with the design requirement and objectives can be found in the final report submitted to the competition [1].

From the preliminary design of Baruna-1 aircraft, the structural components such as skin, rib, spar, longeron, stringer, etc, were sized using the reference data available in [2], [3]. At this stage, no detail analysis to made to determine the size of those components. The MTOM obtained for this aircraft is calculated by assuming a constant dimension of each structural components, regardless of the load exerted on them.

From structural view, increased weight requires stronger structures in order to support the weight, which will also affect the economic aspect of the aircraft. Considering this matter, designers ought to minimize the aircraft's weight while still compatible with safety. That being said, airworthiness regulations stated several factors that the aircraft primary structure must satisfy in order to make sure that

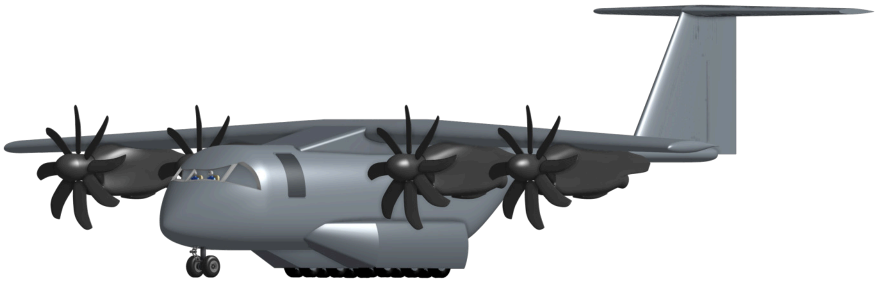

FIGURE 1.1: Baruna-1 Firefighting Aircraft.

the aircraft still complies with the minimum standard of strength and safety. These safety factors consist of limit load, the proof load, and the ultimate load.

In accordance with FAR 25.337, the maneuvering load factor limit was determined that the airplane is considered to be subjected to symmetrical maneuvers, unless limited by maximum lift coefficients under static condition [4]. The design speed of an aircraft must also be in compliance with the FAR 25.335.

The structural configurations of the aircraft must be able to withstand a load of -1 to +3.15, according to the FAR 25. At sea-level and with the maximum take-off weight, the values of the stall speed (V_S), maneuvering speed (V_A), cruise speed (V_C), and dive speed (V_D) were determined to be 54 m/s (177.165 ft/s), 86 m/s (282.152 ft/s), 151 m/s (495.407 ft/s), and 236 m/s (774.278 ft/s), respectively, and the load factor must be multiplied by the safety factor of 1.5 for the ultimate load.

According to the project report of Baruna-1, the dimensions of the main structures of the Baruna-1 (such as the spar, rib, stringer, longeron, and skin) were roughly estimated to support the load below the fatigue strength limit. However, since the design is still in the preliminary stage, all of the values mentioned should be analyzed further in order to prove the calculations before continuing to the next phase which is detailed design considering that some of the values were obtained by estimation [5].

1.2 Research Objectives

The objectives of this research are:

- Analyze the design configuration of the wing structural components of Baruna-1 under the specified static load.
- Determine the dimension wing skin, ribs, and spars that met the requirements given by FAR 25.

1.3 Research Scope and Limitation

The scope and limitation of this research are:

- The analysis is based on the designated configurations made in the previous design process of Baruna-1.
- The analysis was performed only for the static analysis.
- The wing is analyzed under a clean configuration (no flaps).
- The wing is analyzed under zero incidence angle $\alpha_{in} = 0$.
- The total load of wing includes the engine and fuel weights.

1.4 Significance of the Study

The results of this research are expected to:

- Give a recommendation for the wing structural design.
- Improve the existing design before moving to the detailed design phase.

- Provide benchmark sizing for the detail analysis such as FEM analysis.
- Ensure the safety of the design.
- Provide a better overall cost efficiency for the design and development.

CHAPTER 2
LITERATURE REVIEW

2.1 Aircraft Design Processes

In designing an aircraft, there are three stages of the process: the conceptual design phase, preliminary design phase, and detail design phase, as shown in the Figure 2.1 of the design process flowchart. The first stage or also said as the conceptual design is the beginning of the design process. First, the aircraft configurations' initial drawings are made to meet the aircraft's requirements [2], [6]–[8].

The conceptual design was then completed by the preliminary design phase, which optimized the conceptual design to meet the required parameters. Next, some testing and calculations for the current design and the structural assessments are taken to rectify any structural problems and defects before moving on to the final stage of the design process, the detailed design, which is the detail design phase [2], [6]–[8].

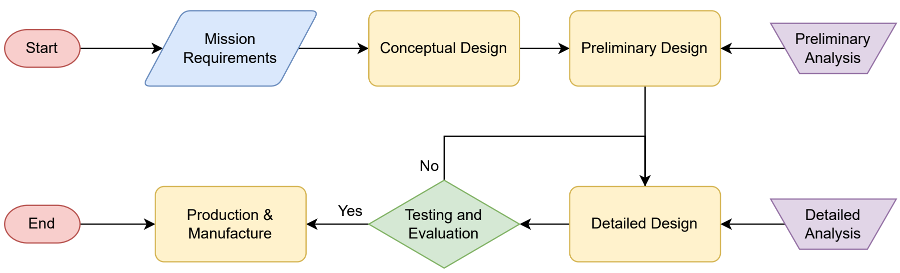

FIGURE 2.1: Aircraft Design Process Flowchart

To design an actual aircraft, the engineers must employ the existing designs. This stage is utilized to develop the concepts made in the previous stages into an operational aircraft. From a structural point of view, it is aimed at the aircraft to be able to sustain the load given by the V-n diagram. Therefore, simulations might also be performed to evaluate and verify that the design could bear the respective loads [6][7].

The complete process of the conceptual design of an aircraft has been implemented on Baruna-1 in the AIAA Aircraft Design Competition for an aerial firefighting aircraft. Baruna-1 aerial firefighting aircraft is designed with a primary mission to combat wildfires while maintaining a low operational cost along with ensuring the aircraft's eminence. The mission profile of Baruna-1 is shown as follow (Figure 2.2):

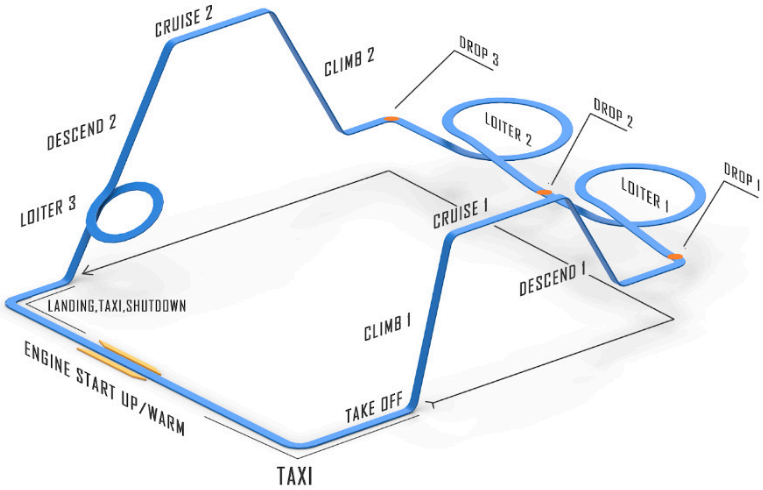

FIGURE 2.2: Baruna-1 Mission Profile

Baruna-1 aircraft has a fire retardant capacity of 8000 gallons, and with a fire retardant reload of 1761 gal/min by using a water pump and 924.6 gal/min by using a vacuum pump, this aircraft aimed to be a powerful firefighting aircraft that could drop eight times at maximum performance with the drop speed of the aircraft is 60 ms^-1. The drop altitude is selectable to 50 m. With maximum fuel capacity, Baruna-1's maximum mission range is 4500 meters, and its maximum ferry range is 12 500 meters [1].

Baruna-1 Aircraft is designed to meet the design requirements and objectives specified by AIAA as shown in Table 2.1.

Since it is part of the design scope, the overall design of the Baruna-1 aircraft can be found in the project report [1].

Code	RFP	Mandatory	Goal
R0	Entry into service (EIS)	Year 2030	Year 2030
R1	Engine readiness year	$\leq$ Year 2028	$\leq$ Year 2028
R2	Specific fuel consumption/efficiency, thrust/power and weight	Assumptions must be documented	
R3	Fire retardant capacity (gal)	4000	8000
R4	Multi-drop capability	Yes	Yes
R5	Volume per drop	$\geq$ 2000	$\geq$ 3000
R6	Fire retardant reload rate	$\geq$ 500 gal/min	750 gal/min
R7	Retardant density	$\geq$ 9 lbs/gal	9 lbs/gal
R8	Drop speed	$\leq$ 150 kts	$\leq$ 125 kts
R9	Drop altitude	$\leq$ 300 ft AGL	150 ft AGL
R10	Design radius with full payload (nmi)	200	400
R11	Design ferry range (kts)	2000	4000
R12	Dash speed (kts)	300	400
R13	Balanced field length	$\leq$ 8000 ft @ 5,000 ft MSL elevation on a +35°F hot day	$\leq$ 5000 ft @ 5,000 ft MSL elevation on a +35°F hot day
R14	Certification	VFR and IFR flight with an autopilot	VFR and IFR flight with an autopilot
R15		Flight in known icing conditions	Flight in known icing conditions
R16		FAA 14 CFR Part 25	FAA 14 CFR Part 25
R17		Autonomous operations	

Table 2.1: Baruna-1 Design Requirements and Objectives

2.2 Aircraft Structural Design

Aircraft loads are the forces and loadings used to analyze the strength of an aircraft's structural components. Such loadings may be caused by air pressure, inertia forces, or ground reactions during landing performances. In addition, design loadings may be used in more complicated circumstances when carrying out other operations, such as catapult take-off or water landing. The design of the structure is affected by the loads. The amount of structural weight involved is one of several factors to be considered when determining the load analysis scope [9].

In addition to giving the aircraft an aerodynamic shape and distributing and withstanding the applied loads of the aircraft, general aircraft structures must also protect the passengers, cargo, fuel, systems, and other payloads during flight. An aircraft's structure must support two types of loads: ground loads, which include all loads encountered while moving or being transported on the ground, such as loads encountered during taxiing, landing, towing, and hoisting. Secondly, the air loads include loads incurred on the structure while in flight by gusts and maneuvers

[5].

Additionally, aircraft are designed for a specific purpose and encounter loads distinctive to that role. For example, an amphibious aircraft that must be able to perform a water landing requires a structure that is stronger than average to sustain the forces during flight under extreme-turbulent air [5].

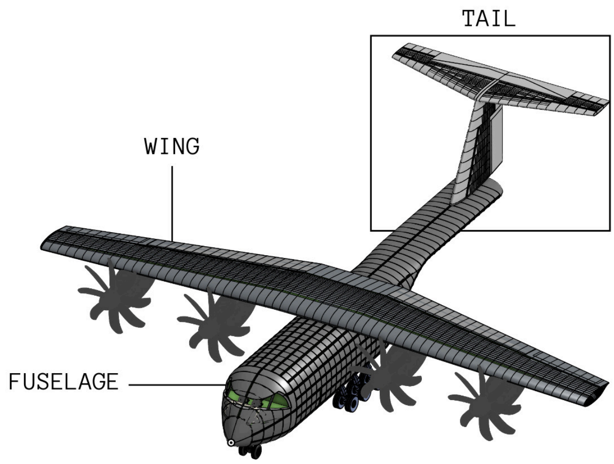

FIGURE 2.3: Aircraft Configuration

These aircraft loads are distributed throughout the aircraft's structural components, which are classified into three main parts: fuselage, wing, and tail, which will be discussed further in this section. Depending on the type of aircraft and its function, the fuselage encloses the crew and the payload, which could be passengers, cargo, weapons, or fuel. The wings provide lift, and the tailplane is primarily responsible for directional control of the aircraft. Mechanical connections and aerodynamic coupling allow these three main parts to engage. Overall, an aircraft's appearance is similar to a metal cage encased in a skin made of aluminum or composite as shown in Figure 2.3 [10][3].

2.2.1 Aircraft Structural Components

Fuselage

Although shaped differently from the aerodynamic surfaces, all sub-structures of the fuselage that perform similar functions to the ones in the wing and aerodynamic surfaces all have the same functions. The fuselage structure is generally a single-cell thin-walled tube consisting of fuselage skin, frames, and stringers. While fuselage skin acts the same as the ones on the wing, longerons act similarly to wing stringers, except longerons are much heavier than wing stringers [5].

Wing

Wings consist of ribs that maintain the aerodynamic cross-section shape for every load combination, distribute and redistribute concentrated loads and stress into the structure, increase the buckling stress of some sub-parts, and resist the distributed loads of aerodynamic pressure on the wing skin [5].

Wing skin mainly carries the structural loads of the wing. The primary function of wing skin is to support the aerodynamic pressure distribution and transmits these forces to the ribs and stringers. Shear stresses created in the skin, spar webs resist shear and torsional loads, while the combination of skin and stringers provides resistance to axial and bending loads [5].

Wing stringers primarily rely on rib attachments to prevent column movements. As mentioned in the previous paragraph, the combined effect of stingers and skin results in resisting axial and bending stresses. On the other hand, spar webs play an essential role in stabilizing the spar flanges or caps with the skin, supporting large compressive loads from axial and bending effects [5][11]. The entire structural components can be seen in Figure 2.4.

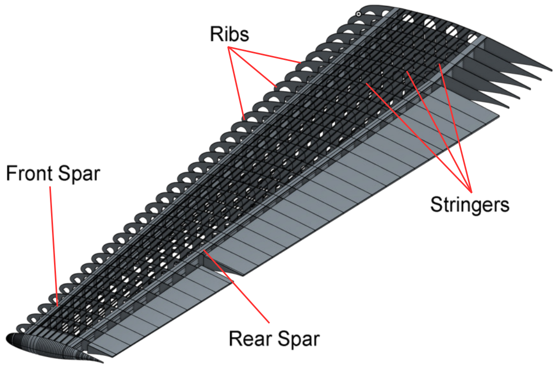

FIGURE 2.4: Wing Structure

Tail

The main loads on the aerodynamic surfaces (tail, fin, and control surfaces) are similar to the wing, except the fin is loaded laterally, inducing fuselage torsion. All of the remarks explained previously are applicable to the aerodynamic surfaces except in some cases (e.g., undercarriage loading, engine thrust, and so forth.) [5].

2.2.2 Wing Load

The pressure distribution on the wing's upper and lower surfaces is determined by the shape of the wing's cross section. Besides to that, the lift force is the integration of the pressure distribution over the wing. Another parameter that is important is the lift coefficient (C_l), which is the balanced lift force by the dynamic pressure and the wing area. C_l is the lift coefficient of the cross section of airfoil, the term of "section lift coefficient" is often utilized to describe the C_l. While the C_L (uppercase L) is often utilized to denote the lift of a 3D wing (the whole wing) [12][13].

It can be seen from the $C_l - \alpha$ graph that the lift coefficient escalates with the angle of attack [13]. The representation of this can be seen on Figure 2.5.

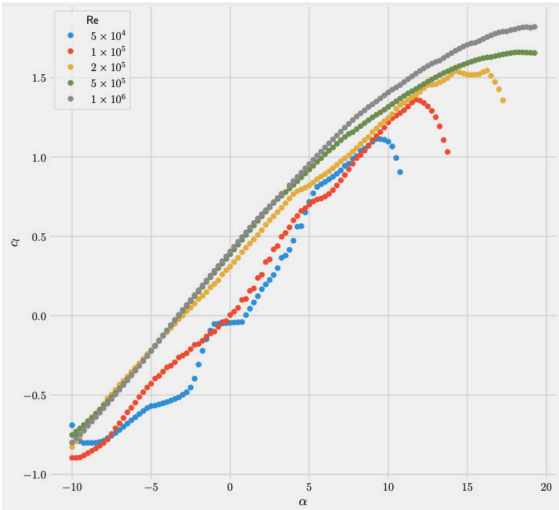

FIGURE 2.5: $C_l - \alpha$ Graph

According to the linear airfoil theory, the lift coefficient of the airfoil section of an infinite wing (2D wing) is linearly proportional to the angle of attack of the wing itself [13]. This relation can be seen through the slope equation of

$$dC_l/d\alpha = 2\pi \text{ (radian)} \tag{2.1}$$

Based on this theory, it is adhered that the generated lift of the wing will increase along with the escalation of the angle of attack, infinitely. However, in practical terms the maximum angle of attack, past which the flow cannot continue the curvature of the airfoil, actually sets a limit on the amount of lift that can be generated [14]. As a consequence, at the certain point of the escalation of the angle of attack, the lift coefficient will reach its maximum and starts declining (as shown in the cl-alpha figure). The lift coefficient at this point is called the maximum lift coefficient [12].

Besides from the angle of attack, the maximum thickness-to-chord ratio ($(t/c)_{max}$) also has a repercussion on the maximum lift coefficient ($C_{L_{max}}$). According to the Figure 2.6, the greatest maximum lift coefficient appears to be happen at $(t/c)_{max}$ $\simeq$ 14% [12].

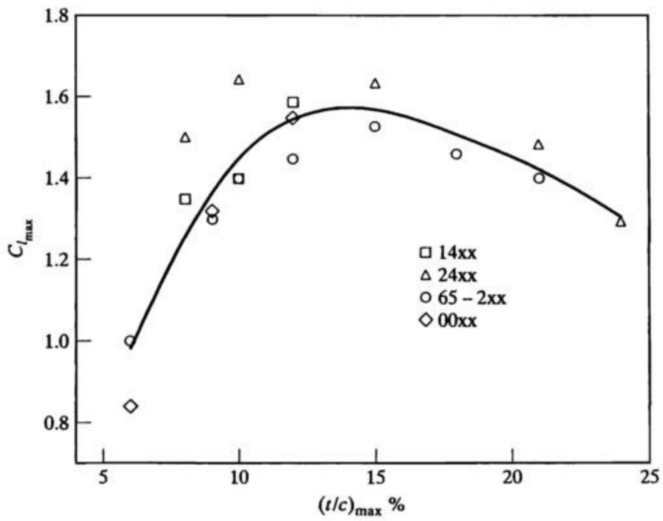

FIGURE 2.6: c_l-t/c Graph

From a structural perspective, utilizing a thicker wing cross section has several advantages to the aircraft. Assuming the wing as a uniform cantilever beam, the maximum deflection is in proportion to the thickness to the third power. Due to this, even a slight increase in wing thickness has a significant beneficial effect on the bending stiffness increment. In result, the elements that carries the wing load can be made lighter which can also reduced the structural weight of the aircraft wing by increasing the $(t/c)max$ while the amount of bending is still the same [12].

Another important parameter in wing design is the taper ratio, which represented as $\lambda = c_t/c_r$, where c_t is the chord at wing tip and c_r is the chord at wing root [12]. The illustration of this can be seen in the Figure 2.7

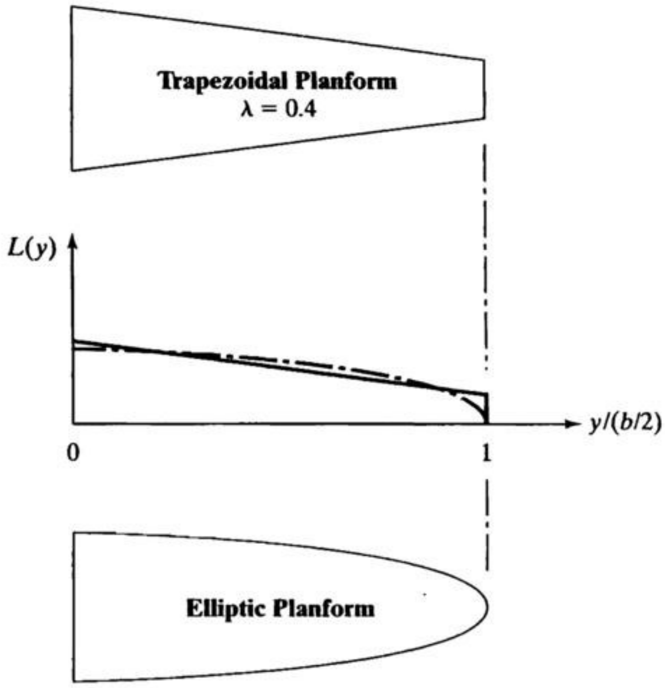

FIGURE 2.7: Wing Planform Shape

The designation of the taper ratio is important in order to minimize the lift-induced drag amount resulted on the wing. According to the lifting line theory, wing design that produces minimum drag is the ellipse shaped wing. With this kind of wing, the lift varies elliptically along the span. A more concise trapezoidal wing with a 0.4 taper ratio can correctly approximate this [12].

A trapezoidal wing's taper ratio, which provides the least amount of lift-induced drag, is slightly contingent with the aspect ratio and more highly by the wing sweep angle [12].

Wing sweep is the angular distance by a line parallel to the center line of the aircraft and either a line linear to the leading edge (Λ_{LE}) or a line perpendicular to the wing's maximum thickness point throughout the span ($\Lambda_{t/c}$). Integrating a sweep angle allows the design to have a greater section critical Mach number (M), and helps reducing the effective Mach number ($M_{effective}$) on the leading edge (LE) which represented by the equation [12]:

$$M_{effective} = M_{\infty} cos \Lambda_{t/c} \tag{2.2}$$

However, integrating sweep to the design comes with some drawbacks including lower lift produced due to low effective dynamic pressure ($q_{effective}$) [12]. This is represented by the equation:

$$q_{effective} = q_{\infty} cos^2(\Lambda) \tag{2.3}$$

Another disadvantage by having a wing sweep is the addition of wing weight [12]. The correlation between them shows on below equation:

$$W_{wing} \propto [tan(\Lambda^2)] \tag{2.4}$$

Additionally, the aircraft could have a poor take off and landing characteristic due to having a large sweep angle. This is the result of a less effectiveness of the lift devices [12].

Historically, for aircraft that have a subsonic cruise Mach number $M_{cruise} \leq 0.4$, the wing designed without a sweep angle (Λ). For aircraft that have a transonic cruise Mach number $M_{cruise} = 1.0$ (mostly commercial aircraft) the sweep angle is added by $\approx$ 30 degrees. For aircraft that have a supersonic cruise Mach number ($M_{cruise} \geq 1.0 to 2.4$, the sweep angles are determined to be close to its Mach line angle [12]. Additionally, for aircraft that are hypersonic ($M_{cruise} \geq 2.4$), the Λ have historically been less than what is required to achieve subsonic flow at the leading edge. The main cause of this is because having an excessively large wing sweep leads to poor subsonic flight characteristics, also an excessive amount of structure weight which is in relation to the theory stated previously [12].

2.2.3 Regulation on Aircraft Load

The safety standards incorporated into every aspect of an aircraft's construction determine its airworthiness. These encompass everything from structural stability to the requirement of specific safety measures in the circumstance of crash landings, as well as design specifications for the electrical, hydraulic, and aerodynamic systems. The decision of the minimum safety standards is primarily the responsibility of the national and/or international airworthiness authorities who designate the official requirement policy documents. These documents includes the requirements of the operational, safety, maintenance and practice, as well as the design requirements [5].

The design of an aircraft is regulated according to the FAR 25 [15] [16], which specified the structural loads as shown below:

§25.335 Design airspeeds.

(a) ***Design cruising speed,*** V_C**.** For V_C the following apply:

1. The minimum value of V_C must be sufficiently greater than V_B to provide for inadvertent speed increases likely to occur as a result of severe atmospheric turbulence.

2. Except as provided in §25.335(d)(2), V_C may not be less than $V_B + 1.32U_{REF}$ (with U_{REF} as specified in §25.341(a)(5)(i)). However, V_C need not exceed the maximum speed in level flight at maximum continuous power for the corresponding altitude.

3. At altitudes where V_D is limited by Mach number, V_C may be limited to a selected Mach number.

[*Doc. No. 5066, 29 FR 18291, Dec. 24, 1964, as amended by Amdt. 25–23, 35 FR 5672, Apr. 8, 1970; Amdt. 25–86, 61 FR 5220, Feb. 9, 1996; Amdt. 25–91, 62 FR 40704, July 29, 1997*]

§25.337 Limit maneuvering load factors.

(a) Except where limited by maximum (static) lift coefficients, the airplane is assumed to be subjected to symmetrical maneuvers resulting in the limit maneuvering load factors prescribed in this section. Pitching velocities appropriate to the corresponding pull-up and steady turn maneuvers must be taken into account.

(b) The positive limit maneuvering load factor n for any speed up to V_n may not be less than $2.1 + 24,000/(W + 10,000)$ except that n may not be less than 2.5 and need not be greater than 3.8-where W is the design maximum takeoff weight.

(c) The negative limit maneuvering load factor-

1. May not be less than -1.0 at speeds up to V_C; and
2. Must vary linearly with speed from the value at V_C to zero at V_D.

(d) Maneuvering load factors lower than those specified in this section may be used if the airplane has design features that make it impossible to exceed these values in flight.

Doc. No. 5066, 29 FR 18291, Dec. 24, 1964, as amended by Amdt. 25–23, 35 FR 5672, Apr. 8, 1970

This regulation is synthesized and implemented in the analysis as $V-n$ diagram. For Baruna-1 aircraft configuration, this diagram is shown in detail in Section 3.2.

2.3 Static Structural Analysis

As mentioned from the previous section, all of the general components of an aircraft must be able to sustain the normal and shear stress from various statics and dynamics loading [17][14]. This study analyzes the static loading of an aircraft, consisting of shear force, bending moment, and torsion, which are discussed in more detail in this section.

2.3.1 Shear Force

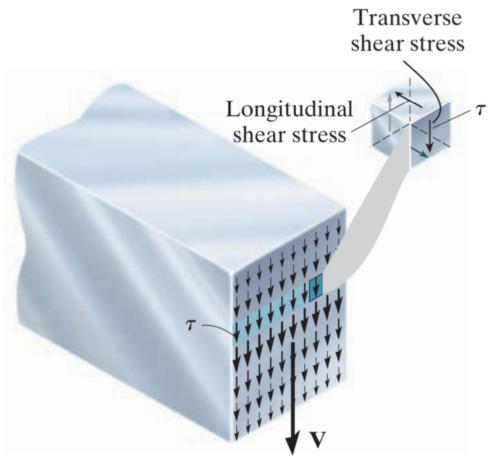

FIGURE 2.8: Shear Stress Schematic [18]

Shear forces act tangentially to a surface, while the vertical shear loads at wing root helps sustain the weight of the rest of aircraft main structures. Thin panels and stiffeners used in the aircraft reacted to shear within the aircraft structure in order to prevent buckling at a higher shear load [5].

The occurrence of shear indicates the presence of bending loads, which causes the beam to deform into an inverted 's' shape. In beams with small cross-sectional dimensions in respect to its length, the shear stress is fairly low. Therefore, the basic theory of bending may still be applied with reasonable accuracy. However, the condition would be different in thin-walled sections. The shear stresses produced in thin-walled sections are not considered small, thus, it has to be evaluated even though the direct stresses may still be determined by using the basic theory of bending by eliminating the axial constraint stresses [5][17].

The general equation of the shear stress is shown in the equation of:

$$\tau = \frac{QV}{Ib} \tag{2.5}$$

Where V is the total shear force at specific location (Nm), Q is the first moment of area (m^3), I is the moment of inertia (m^4, and b is the width of the member [19].

2.3.2 Bending Moment

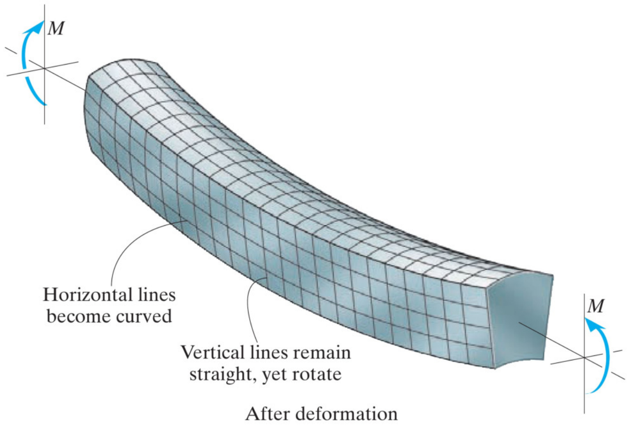

FIGURE 2.9: Bending Moment Schematic [18]

Uniform direct stress across the cross section of the member produced when an axial load is applied. However, when the applied loads are vertical, it will bring a different situation to the beam which will cause the beam to bend and form a sagging or hogging shape. If the beam sags, the upper sections of the beam will become shorter than the lower sections (the principle for hogging will be in reverse), this means the strains in the upper and lower sections will be different. Since the stress is directly proportional to the strain, stress then will vary with the depth of the beam [5].

The bending stress can be calculated by the general equation of:

$$\sigma_b = \frac{My}{I} \tag{2.6}$$

Where σ_b is the bending stress (Pa), M is the bending moment at certain point (Nm), y is the perpendicular distance between neutral axis and certain point (m), and I is the moment of inertia of the section about the neutral axis [19].

Symmetrical bending occured in beams with single or double symmetrical cross-sections (as shown in figure). The length of the beam will bend into a concave at upper surface and convex at lower surface. As a result, direct stress changes along with the depth of the beam, from compression in the upper fibers to tension in the lower fibers. Nevertheless, there will be a certain area where the fibers do not change in length, this means the direct stress is zero at that certain point (also called a neutral plane). Therefore, there will be a difficulty in determining the variations in direct stress over the depth of the beam, the stress values, and the corresponding beam deflection [19]. In order to evaluate the direct stress distribution (pure bending), some primary assumptions are applied which are: after bending, the plane cross-sections of the beam remain normal to the longitudinal fibers of the beam, and that the beam's materials are linearly elastic and homogenous [5].

Increases in angle of attack result in an upward aerodynamic force component perpendicular to the plane of the wing, which deforms the wing generally. It can be demonstrated that within a civil aircraft's flight envelope, this normal force is slightly less than lift. As a result, it is conceivable to calculate the bending load using lift rather than the normal pressure force component [20].

Utilizing the character of thin-wall on aircraft structures, some assumptions could be made to simplify the determination of bending loads and deflections. As a result, the thickness (t) of a thin-walled section is considered to be small in comparison to the actual cross-sectional dimensions, allowing the stresses to be considered as constant across the section [5].

2.3.3 Torsion

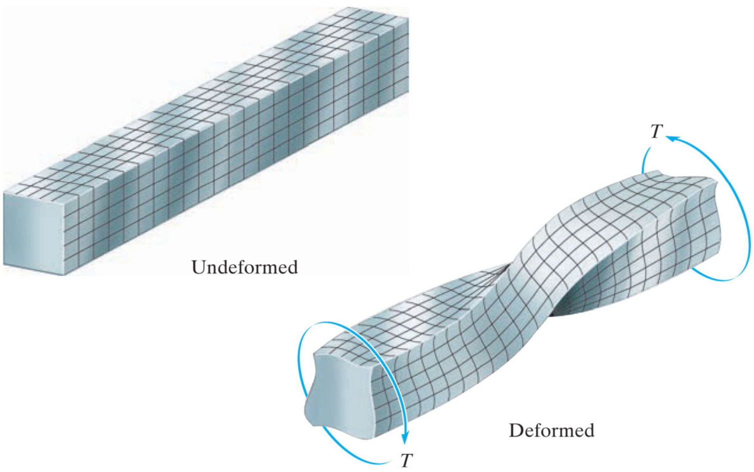

FIGURE 2.10: Torsion Schematic [18]

Lightweight structures, such as those found in aircraft, are often constructed of thin-walled tubes with non-circular cross-sections. In some applications, they may be subjected to torsional loading [18].

Torsion can be reacted either by shear stresses or by differential bending of beams positioned about an axis of twist, and the most efficient shape for carrying torsion is a thin-walled cylinder of the greatest possible diameter [5].

From the equation of shear stress related to torsion, the equation of torque is obtained as follows [19]:

$$\tau = \frac{T\rho}{J} \tag{2.7}$$

Where τ is the shear stress (Pa), T is the torque acting on the member (Nm), ρ is the distance between the neutral axis to the certain point where the shear stress is acting (m), and J is the polar moment of inertia of the member (m^4).

2.3.4 Static Load on Wing Structure

According to Lomax [21], some considerations are given to the net loads during the structural analysis of the wing box. Before the advent of finite element methods, the conventional method of analysis for wing stress was based on beam theory at a section normal to the wing box. In this case, the net loads are summed to determine the shear, moment, and torsion along a selected reference axis [14]. On the other hand, by using the finite element method for wing stress analysis, the generated aerodynamic loads as well as the internal loads brought on by inertia in the wing should be distributed in a predetermined way on the wing structural model [21].

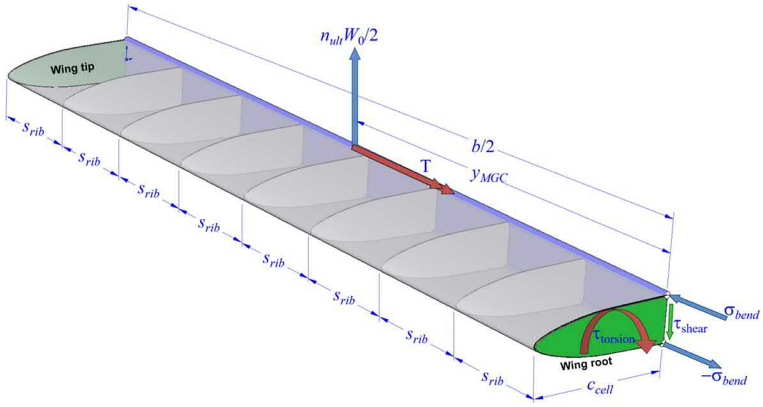

FIGURE 2.11: Forces Acting on Wing

According to Snorri [22], the critical loads acting on the wing structures can be mathematically represented as:

$$\begin{aligned} V &= n_{ult}W_0/2 \\ M &= \frac{n_{ult}W}{2} \times y_{MGC} \\ T &= \frac{1}{2}\rho V_\infty^2 \frac{S}{2} \cdot c_{MGC} \cdot C_m \end{aligned} \tag{2.8}$$

Where V, M, T are the shear force acting on the wingspan, the bending moment at the wing root, and the torsion at the wing root, respectively. This is illustrated in Figure 2.11. In this study, the $n_{ult}W_0$ will later be replaced with the total load of Baruna-1 aircraft.

2.3.5 Fuel Tanks Effect on Wing Loads

In determining the overall wing loading distributed throughout the span (summed airloads and inertia loads), one of the element that need to be considered is the fuel effect on the wing. Especially if the aircraft is designed with multiple fuel tanks distributed across the wings and fuselage, which could have a significant impact on the design load [21].

The fuel tank placement was also taken into account in order to optimize the load relief from inertia such that the fuel used is the one from the center wing tank before using the fuel on the outer tank of the wing. As a result, a fuel pump is required to be integrated in the center wing tank to keep the outer tank full until the fuel in the center tank runs out [21].

CHAPTER 3
RESEARCH METHODOLOGY

This section starts by explaining the configuration of Baruna-1 aircraft, especially the wing structural component and its dimension that are used as a reference to compare in the Chapter 4. After that, the analysis tools are described thoroughly. At the end, the process are summarized in the final subsection.

3.1 Baruna-1 Aircraft

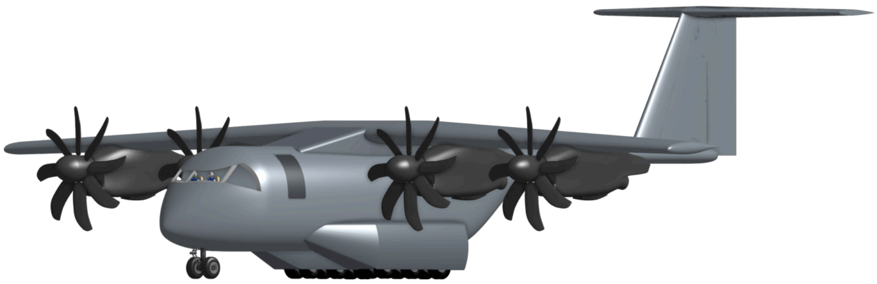

Figure 3.1: Baruna-1 Full Configurations.

The configuration of the Baruna-1 Aircraft design were obtained based on the calculation of design indexes. The final optimum configurations for the aircraft are shown in Table 3.1.

TABLE 3.1: Baruna-1 Design Configurations Cont.

No	Configuration	Selection
1	Type	Conventional
2	Propulsion	Turboprop
3	Number of Engines	Double twin-engine
4	Engine and Aircraft CG	Tractor
5	Engine Installation	Fixed
6	Engine Location	Under wing
7	Number of Wings	One-wing
8	Wing Geometry	Tapered
9	Dihedral Angle	Non-dihedral
10	Wing Sweep	Fixed sweep angle
11	Wing Setting Angle	Fixed setting angle
12	Wing Placement	High-wing
13	Wing Installation	Cantilever
14	Wing Control Surfaces	Aileron and Flap
15	High-lift Devices	Trailing-edge flap
16	Wing-tail Control Surfaces	Conventional (elevator, aileron, and rudder)
17	Tail or Canard	Tail
18	Tail Shape	T-tail
19	Vertical Tail (VT)	One VT at Fuselage
20	Horizontal Tail Control Surfaces	Adjustable horizontal tail
21	Vertical Tail Control Surfaces	Vertical tail and rudder
22	Power System	Fly-by-wire
23	Landing Gear Type	Multi-bogey
24	Shock Absorber	Oleo pneumatic
25	Landing Gear Layout	Dual twin tandem
26	Landing Gear	Retractable
27	Fuselage	Single long-fuselage

Baruna-1 Design Configuration		
No	**Configuration**	**Selection**
28	Material for Structure	Full metal
29	Equipment Installation	Semi modular
30	Water Collection	Land tanker
31	Number of Payload Tanks	Multi-tank
32	Pump System	Hydraulic pump
33	Pressure Delivery System	Bleed air
34	Tank Internal Structure	Unbaffled
35	Tank Material	Stainless steel
36	Tank Head Shape	Semi-ellipsoidal
37	Payload Tank Shape	Cuboid
38	Retardant Delivery System	Pressurized tank system
39	Situational Awareness	Conventional + Thermal Imaging Devices

3.1.1 Baruna-1 Aircraft Configuration

Baruna-1's initial sizing were made according to the fixed design explicated in the previous section [1]. As the design were still in the preliminary stage, the sizings and weight were measured roughly according to the design requirements. Table 3.2 to 3.3 shows the definite specifications of the aircraft sub-structures.

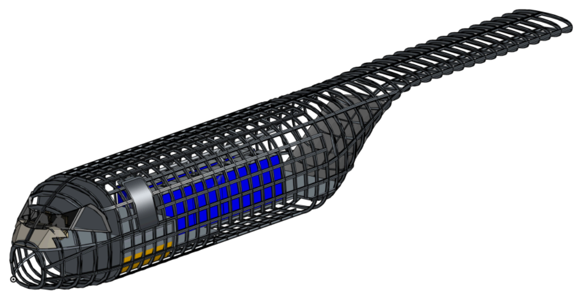

(A) Fuselage Substructure

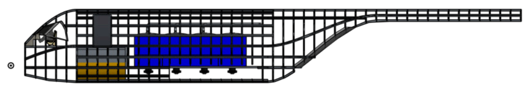

(B) Side-view

FIGURE 3.2: Baruna-1 Fuselage Substructures.

Baruna-1 Fuselage Sizing		
Part	**Sizing (mm)**	**(in)**
Frame Spacing	558.88	22.003
Frame Depth	74.471	2.932
Longeron Spacing	12	0.472
Skin Thickness	0.35	0.014
Fuselage Length	32780	1290.551
Fuselage Height	4500	177.165
Fuselage Width	5000	196.850

TABLE 3.2: Baruna-1 Fuselage Sizing

Baruna-1's tail structural sizings were identical with the ones on the wing as shown in Figure 3.3. The overall tail sizings are specified in Table 3.3.

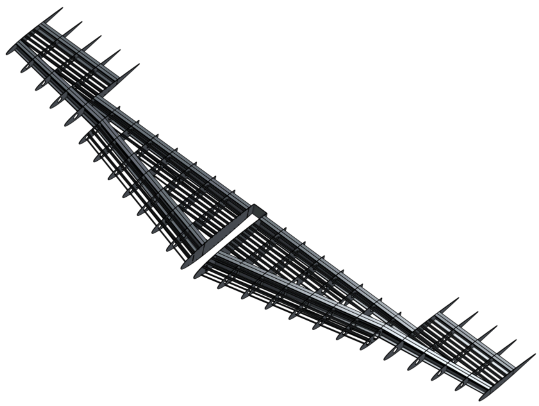

(A) Horizontal Tail

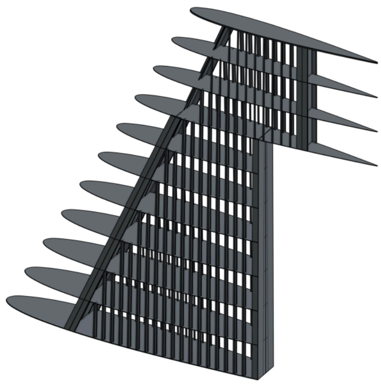

(B) Vertical Tail

FIGURE 3.3: Baruna-1 Tail Substructures

Baruna-1 Tail Sizing		
Part	**Sizing (mm)**	**(in)**
Rib Spacing	600	23.622
Rib Thickness	1	0.039
Stringer Spacing	152.4	6.0
Skin Thickness (Uniform)	0.8	0.031
Spars Web Thickness	1	0.039
Spars Flange Thickness	3	0.118
Stringers Thickness	1.5	0.059

TABLE 3.3: Baruna-1 Tail Sizing

Below Table shows the sizing of Baruna-1 wing structural parts. According to the calculations made, the number of spars and longerons needed were determined. Two spars and 14 longerons are added to the wing structure, and the spar locations are set at 0.2c and 0.65c for the front spars and rear spars, respectively [1]. The sub-structures of Baruna-1 wing design is shown in the Figure 3.6.

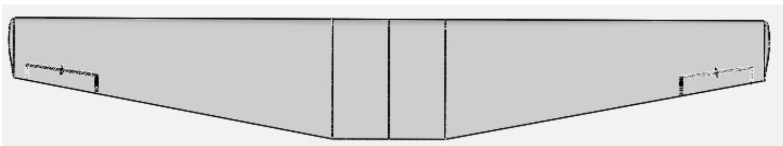

FIGURE 3.4: ST4 with Wingbox MS(1)-0317

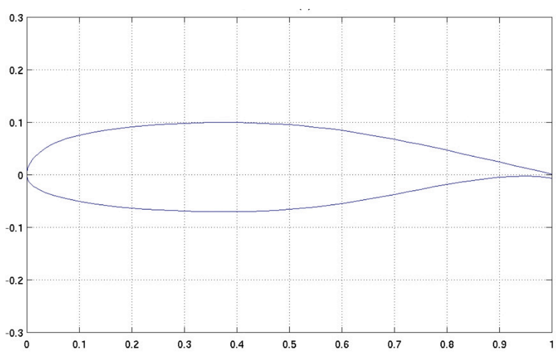

FIGURE 3.5: MS(1)-0317 Airfoil

The aerodynamic parameters of the wing that are obtained from OpenVSP can be seen on Table 3.4.

According to the initial sizing of Baruna-1, the wing planform area of the aircraft approximately is 200 m^2 for 144 560 kg (318 754.8 lbm) maximum take-off mass (MTOM). Baruna-1's aspect ratio (AR) is designated as AR = 8. This value was determined based on the other competitors in which the AR are usually between 8-10 for a subsonic turboprop engine driven aircraft. Correspondingly, the wingspan of the aircraft is determined as 40 m, while the taper ratio of the wing (λ) were determined according to the wing's elliptical lift distribution, which in result, the taper ratio of Baruna-1 is $\lambda = 0$. [1]. The wing parameters are shown in Table 3.4.

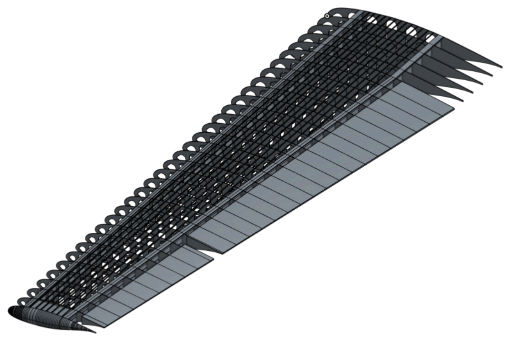

FIGURE 3.6: Baruna-1 Wing Substructure

Parameter	Value	Unit	Value	Unit
Wing Planform Area (S_{ref})	200.00	m^2	2152.8	ft^2
Wing Span (b)	40.02	m	131.30562	ft
Aspect Ratio (AR)	8.00			
Taper Ratio (λ)	0.50			
Twist Angle	-2.00	deg		
Dihedral Angle	-2.00	deg		
Rib Spacing	600	mm	23.622	in
Rib Thickness	1	mm	0.039	in
Stringer Spacing	152.4	mm	6.0	in
Skin Thickness (Uniform)	0.8	mm	0.031	in
Spars Web Thickness	1	mm	0.039	in
Spars Flange Thickness	3	mm	0.118	in
Stringers Thickness	1.5	mm	0.059	in

TABLE 3.4: Baruna-1 Wing Sizing and Parameters

Based on the parameters tabulated in Table 3.4, some potential selections of wing design for Baruna-1 are determined. The most fitted design for Baruna-1 out of all selections is the ST4 with wingbox with MS(1)-0317 airfoil. This decision were considered since the ST4 Wingbox is more voluminous. With a volume of 119.52 m^3, this wing design could provide more space to carry larger amount of fuel in the wing [1].

3.1.2 Materials

The materials used on Baruna-1 structural parts consists of metallic alloys. The material specifications such as Young's Modulus E, yield stress σ_y, and ultimate stress σ_{ult} for Baruna-1 substructures are tabulated in Table 3.5 [23][24].

Baruna-1 Structures Material Specifications					
Structure	**Substructure**	**Material**	E **(GPa)** [24]	σ_y (MPa)	σ_{ult} (MPa)
Fuselage	Skin	AL 2024	73.1	324	469
	Frame	AL 2024	73.1	324	469
	Longeron	Titanium Alloy Grade 5	113.8	830	900
	Stringer	Titanium Alloy Grade 5	113.8	830	900
Wing	Skin	AL 2024	73.1	324	469
	Rib	AL 2024	73.1	324	469
	Spar	AL 2024	73.1	324	469
	Stringer	Titanium Alloy Grade 5	113.8	830	900
	Wing Mounting	AL 2024	73.1	324	469
Tail	Skin	AL 7075	71.1	434	572
	Rib	AL 7075	71.1	434	572
	Stringer	AL 7075	71.1	434	572
	Spars	AL 7075	71.1	434	572
Wheel Housing	Skin	AL 2024	73.1	324	469
	Rib	AL 2024	73.1	324	469

TABLE 3.5: Baruna-1 Structures Material Specifications

Although the substructure sizings of the aircraft tail are identical with the ones on the wing, the materials used for the structural parts between the tail and the wing are different. This is due to the stress at the tail would be higher than the wing, so that a much stronger material is chosen for the tail structural parts [1], [18].

3.1.3 Fuel Tank

The aircraft's fuel tanks are distributed throughout the wing span as shown on the Figure 3.7. Considering that the aircraft is not a passenger carrier, the midsection of the fuselage will only carry the retardant tank. Hence, to maximize the space another fuel tank is placed in the bottom part of the fuselage. The fuel tanks that are located across the wing span are considered as the primary fuel tank, while the one in the fuselage is considered as the secondary fuel tank [1].

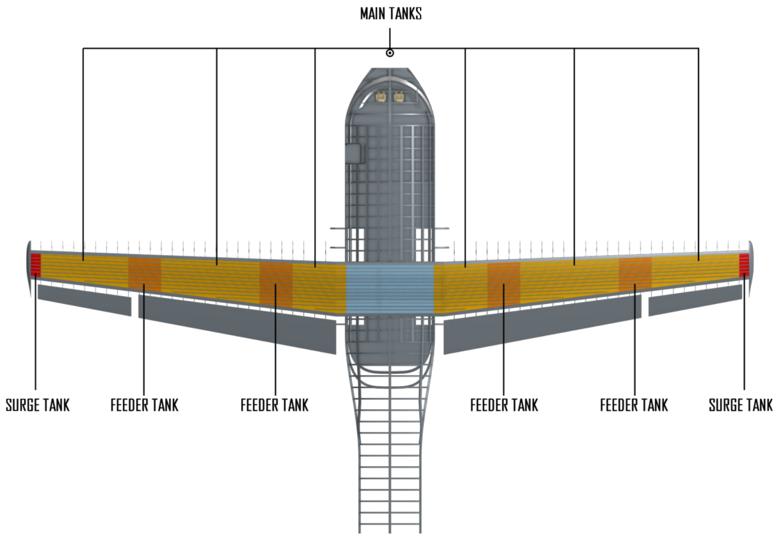

FIGURE 3.7: Fuel Tanks Across the Wing

3.1.4 Aircraft Weight

According to the design configuration, in addition to the wing structures of the aircraft, the engine also contributes to the load on the wing because it is mounted under the wing. Based on the initial sizing analysis of Baruna-1, the P/W of the aircraft design for 144 560 kg (318 754.8 lbm) MTOM is approximately 0.31. From this number, the required power for the aircraft to be able to perform the aimed mission is 46 500 kW (or equals to $\sim$ 35 000 hp). After some considerations, including the manufacturer support and technology, the selected engine for Baruna-1 Aircraft is the Europrop TP400-D6. Excluding the fluid and instrumentation, the weight of the engine is approximately 1960 kg. The length of the engine is 4.18 m measured from the front to the back of the primary nozzle, and the radius of the engine is approximately 1.218 m from the center at the lowest point [1]. The detail configurations of the engine are tabulated on Table 3.6.

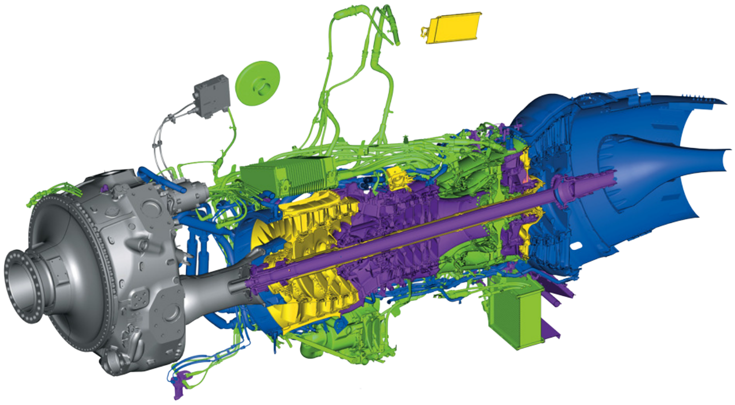

FIGURE 3.8: Europrop TP400-D6 Engine Schematic

Weight and Dimensions		
Weight	1,960	kg
Length	3.5	m
Overall Length	4.18	m
Diameter	1.218	m

TABLE 3.6: Europrop TP400-D6 Engine Configurations

The overall comprehensive weight data of all aircraft components are shown in Table 3.7

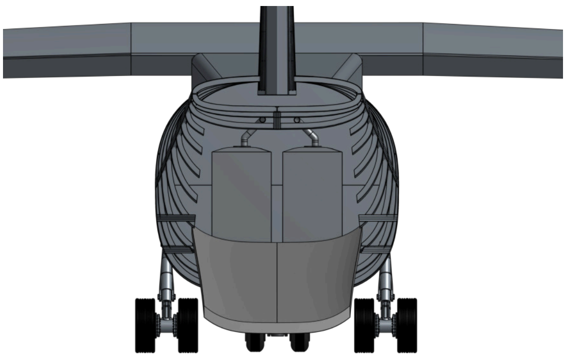

FIGURE 3.9: Baruna-1 Rear Cargo Door

No	Components	Weight (kg)
1	Engine (x4)	7,840.0
2	Landing Gears (Nose and Main)	5,116.0
3	Retardant System	6,863.0
4	Retardant	36,800.0
5	Fuel Tank (Wing)	568.891
6	Fuel (Wing)	30,611.969
7	Fuel Tank (Fuselage)	182.307
8	Fuel (Fuselage)	20,609.851
9	Fuselage Substructure	24,782.61
10	Fuselage Skin	153.899
11	Main Horizontal Wing Substructure (Aileron, etc.)	3,290.221
12	Main Horizontal Wing Skin	917.272
13	Tail Horizontal Wing Substructure	1,139.376
14	Tail Horizontal Wing Skin	
15	Tail Vertical Wing Substructure	609.802
16	Tail Vertical Wing Skin	
17	Rear Cargo Door	31.001
18	Fuselage Door	27.112
19	Wing Mounting	109.271
20	Wheel Housing	1,110.422
21	Air Conditioning Deicing System Weight (W_{api})	1,010.18
22	Auxiliary Power Unit Weight (W_{apu})	566.172
23	Electrical System Weight (W_{els})	332.392
24	Flight Control System Weight (W_{fc})	683.569
25	Instrumentation, Avionics, and Electronics System Weight (W_{iae})	591.965
26	Paint Weight (W_{pt})	424.628
27	Crew x2	162.0
28	Pilot Seat x2	26.1
Total		**144,560.0**

Table 3.7: Baruna-1 Aircraft Component Weight Overall Data

3.2 Aircraft Load for Analysis

3.2.1 Load Factor

During steady-level flight, the weight of the airplane mainly supported by the lift produced by the wing. However, due to additional loads enforced during maneuvers, the overall load acting on the aircraft structures will change either increases or decreases depending on the turbulence or maneuvers. The magnitude of these loads are calculated with the term of *load factor* [9][4].

Load factor or denoted as n is the ratio between the lift and the aircraft weight, which is shown by:

$$n = \frac{L}{W} \tag{3.1}$$

The load factor considered in this study is 3.15, therefore all the wing loads in the calculations of the wing structures are multiplied by the load factor of $n = 3.15$.

The maximum loads that can be expected to be imposed to be placed on the aircraft during its service life are known as limit loads. The structure of the aircraft must be able to withstand the maximum loads without having to suffer damaging structural failure. In addition, the deformation of the structure must be such that it does not impair the safe operation of the aircraft for any loads up to the limit. The ultimate loads or design loads are represented by **Ultimate load = Limit load × Factor of safety** [9].

The ultimate safety factor is generally 1.5. As stated by the requirements, the structure must be able to support this load capacity without failing. Despite the fact that aircraft are not meant to be loaded above their specified limiting loads, nearly every part of the structure is built with a reserve of strength in case a component completely fails structurally. This is caused by a number of reasons, including the approximations in the theories of aerodynamics and structural stress analysis, variations in the physical characteristics of materials, and different standards for manufacturing and control. The fact that almost every aircraft has a maximum speed and acceleration limit to which it can be applied during flight or landing may be the most crucial factor affecting aircraft safety [9].

It is possible for the limit loads to be slightly exceeded in emergencies because of the aircraft controls of the pilot. However, due to the safety margin against failure, this exceeding of the limit load should not pose a significant risk to the safety of the flight, even though it might cause structural deformation that would require replacing or repairing minor components of the structure or small components [9].

3.2.2 V-n Diagram

V-n diagram is generally used to represent the airworthiness requirement of load factor as shown in Figure 3.10. According to the certification specification of EASA specified on CS-25.337, the load factor for an aircraft with an MTOM $\geq$5700 kg and $\geq$22 690 kg of aircraft weight, the load factor is $n = 2.5$. and $n = 3.1$ for aircrafts with the weight of 6350 kg [25].

Figure 3.10 represents a variety of velocities and loads corresponding to the flight cases as well as the range of maneuvers. A diagram similar to the V-n diagram, representing the gust envelope is also utilized to describe the airworthiness requirements for the airflow effects to which the aircraft is most likely to be subjected [25].

Air currents or gusts have an accelerating effect and increase apparent weight in exactly the same way as ordinary maneuvers. They can also act in any direction and generally increase in strength with higher speeds [25].

In accordance with the regulations, the limit load factor have to be in compliance with the FAR 25.337, while the design speed should be in compliance to the FAR 25.335. Figure 3.10 shows the V-n diagram of Baruna-1 with a note that the values were examined at sea-level condition with the maximum take-off weight [1].

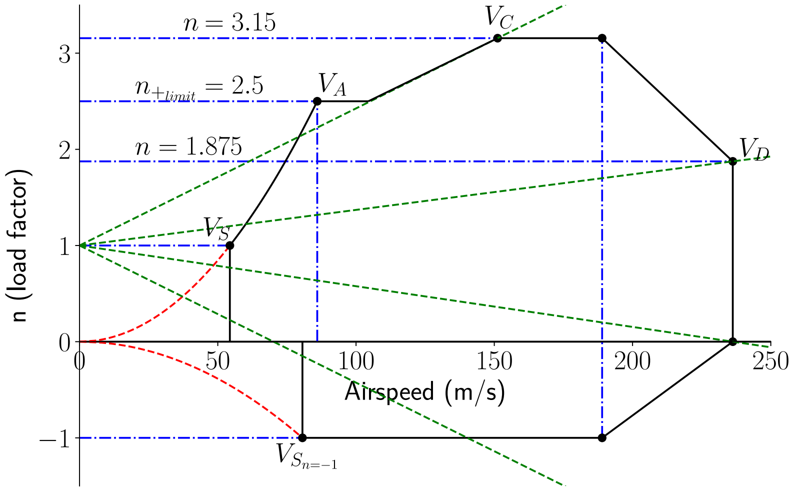

FIGURE 3.10: V-n Diagram at Sea-level Condition

All parameters of the diagram can be seen in Table 3.8.

Baruna-1 V-n Diagram Parameters		
Parameter	**Value** (m/s)	**(ft/s)**
Stall Speed (V_s)	54	177.165
Maneuver Speed (V_A)	86	282.152
Cruise Speed (V_C)	151	495.407
Dive Speed (V_D)	236	774.278

TABLE 3.8: V-n Diagram Parameters

As stated in the FAR 25 [15] [16], the type of aircraft which Baruna-1 complies to should be able to sustain -1 to +3.15 load and the ultimate load is the result from multiplication of the load factor and the safety factor of 1.5. Hence, Baruna-1's main structures' dimensions were deemed to be to withstand the load under the limit of the material's fatigue strength. For Baruna-1 aircraft, the maximum load are located at the fuselage center of mass, the retardant tank areas, and in the middle of the wing's half span [1].

3.2.3 Analysis Method and Tools

CAD Drawing

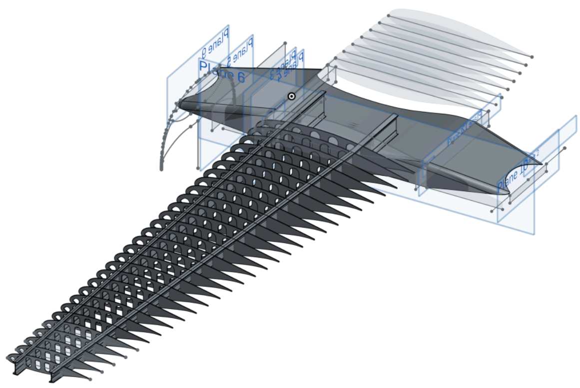

FIGURE 3.11: OnShape CAD Drawing

OnShape is an open-source computer-aided design (CAD) software delivered by a software as a service model (SAAS) which allows the user to utilize a cloud-based applications on the internet. With that being said, the datas computed by using OnShape (such as drawings, structural data, and so forth) are stored on the cloud. The software also allows the user to connect and interact with other users to facilitate a group project and assessments.

The existing 3D drawing of Baruna-1 aircraft was made according to the obtained information from Bruhn [3] and historical datas from Roskam[2]. The geometric datas such as the volume, area, length, height, and other specifications are obtained by using the measurement features on the existing 3D drawing of Baruna-1 aircraft.

OpenVSP

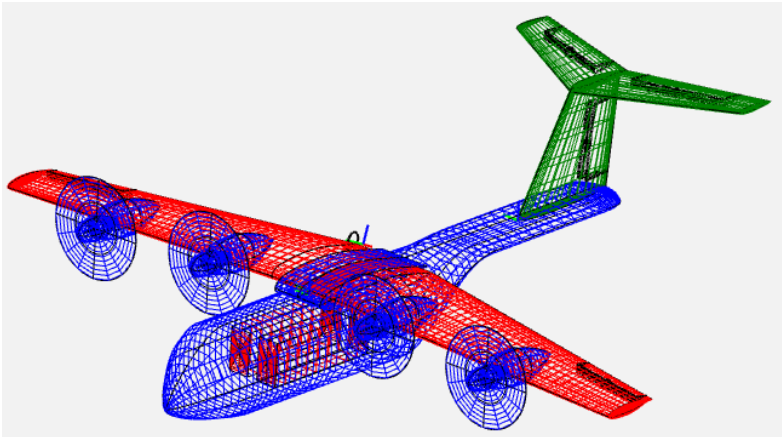

FIGURE 3.12: Baruna-1 Mesh from OpenVSP Software

In addition to the 3D Drawing, several data especially the aerodynamic parameters are obtained from OpenVSP software. OpenVSP is a parametric geometry tools specifically for aircraft models that can be utilized to create an aircraft 3D model as well as supporting some engineering analysis of the model.

From the 3D model of Baruna-1 aircraft as shown in Figure 3.12, the obtained c_l distribution data along the span is shown as follows:

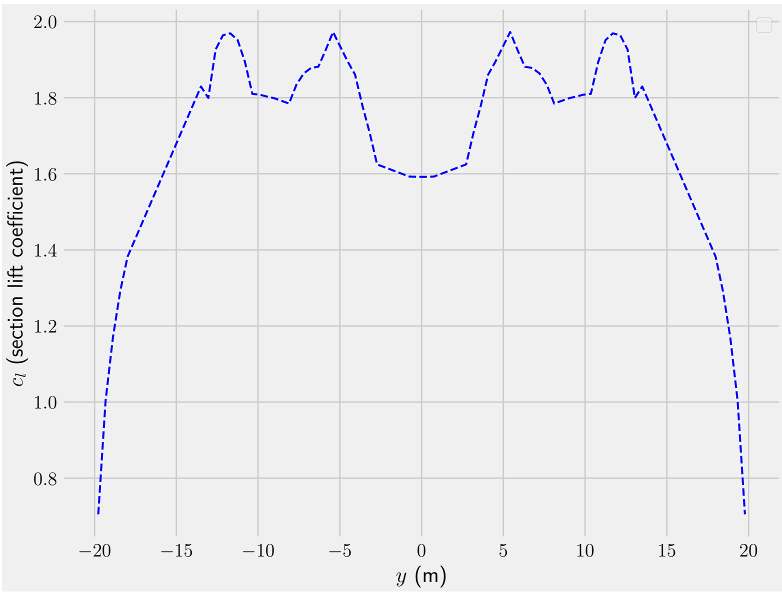

FIGURE 3.13: Baruna-1 c_l Distribution Along the Span at $\alpha = 0$

Spreadsheet

After obtaining the required datas, all of the calculation and analysis of the wing structural design of Baruna-1 aircraft in this research are conducted by using Microsoft Excel spreadsheets which is part of the Microsoft Office suite. The datas obtained by the previous analysis of Baruna-1 are processed by using the basic operation features of the software including the charts which is generated from the specific cell groups.

3.3 Methodology

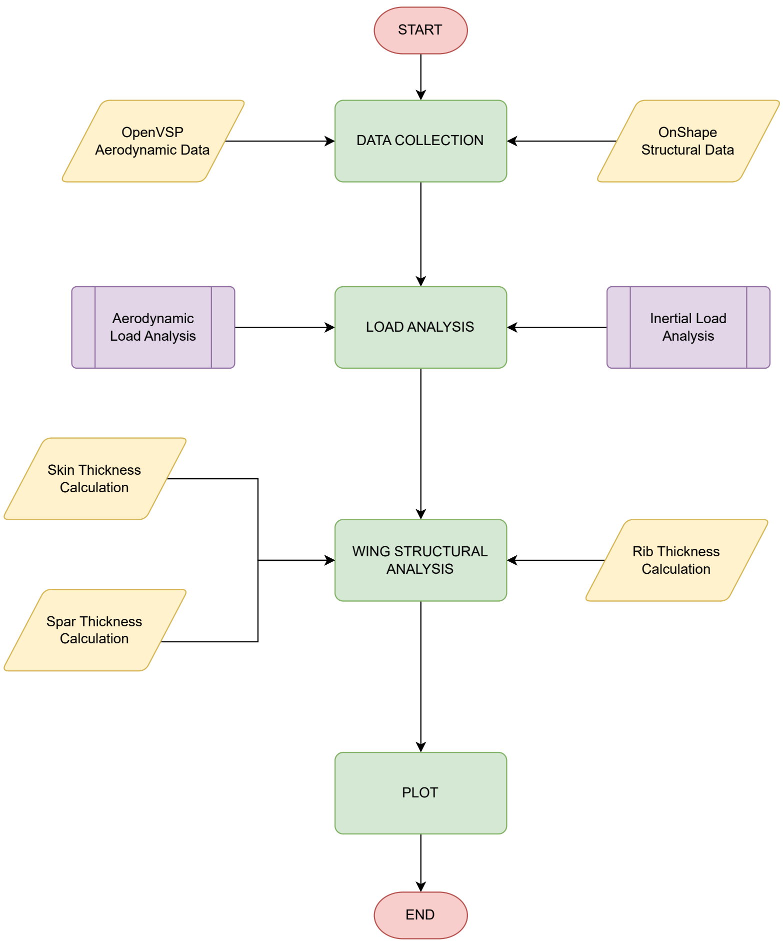

FIGURE 3.14: Research Process Flowchart

Figure 3.14 shows the flowchart of the research process of this study. The first process is data collection. The datas were obtained from OpenVSP for the aerodynamic data and OnShape for the structural data. After the required data was collected, the load analysis was performed by dividing it into aerodynamic load analysis and inertial load analysis. After the total load of the wing is determined, the structural analysis of the wing is performed to obtain the substructure variables, i.e., skin thickness, spar thickness, and rib thickness.

3.3.1 Wing Loading Analysis

Skin Thickness

The required skin thickness along the wing span varies depending on the load distribution. As the load decreases toward the tip of the wing, the skin thickness is also decreases. Therefore, the ideal skin thickness required need to be calculated.

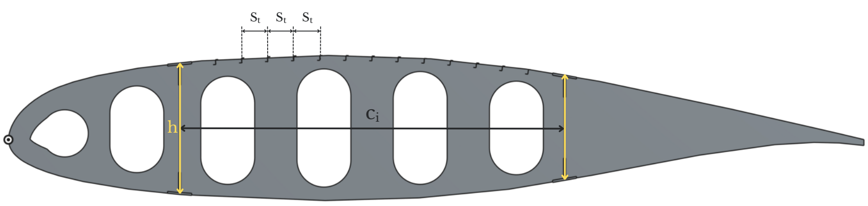

FIGURE 3.15: Wing Box Geometry

In calculating the skin thickness, some parameters has to be determined including the compressive load (the parameters used in the calculations are represented in Figure 3.15) [14]. Compressive load is the result of an axial force acting on a member [18]. Since the aircraft wing is treated as a beam, the span is subjected to axial force [9]. Therefore, the compressive load acting on each wing station could be calculated by:

$$N_i = \frac{M_z}{c_i h_s} \tag{3.2}$$

Where M_z is the bending moment along the span in Newton, c_i is the wing box chord in meters, and h_s is the spar height in meters.

Since there are two spars designated to the wing, the spar height were measured by calculating the average height of both spars [14] by:

$$h_s = \frac{h_1 + h_2}{2} \tag{3.3}$$

After the compressive load is obtained, the skin thickness then could be calculated by substituting the load into the equation shown below:

$$t_{skin} = \left[\frac{N_i (S_t)^2}{3.62E}\right]^{\frac{1}{3}} \times 1000 \tag{3.4}$$

Where t_{skin} is the skin thickness in mm, S_t is the stringer spacing in meters, and E is the modulus of elasticity (Young's modulus) in Pa [9].

Spar Thickness

In addition to the thickness of the outer skin, the thickness of the spar must also be analyzed. The thickness of the spar varies across the wing span, just like the skin thickness. Since it is one of the substructures that mainly supports the wing, the spar thickness must ideally be calculated so that the structure can sustain the load acting on the wing [9].

Since the spars are subjected mainly by torsion, the torque acting on the spar along the span need to be calculated first [14]. In relation to the moment coefficient of the wing, the torque could be represented as [13]:

$$T = M = \frac{1}{2}\rho_\infty V_\infty^2 S_i c_m c_i \tag{3.5}$$

Where the ρ_c is the air density during cruise condition which equals to 0.6601 kg/m^3, V_c is the cruising velocity of the aircraft which is 151 m/s, the S_i is the area section between the wing stations (in m), c_m is the moment coefficient per unit span, and c_i is the chord length of each stations.

Since Baruna-1 is designed with a tapered wing as shown in Figure 3.16, the area section of the wing (S_i) could be calculated by using the area of trapezoid formula since the geometry of the wing is a trapezoidal shape as shown in Figure 3.17.

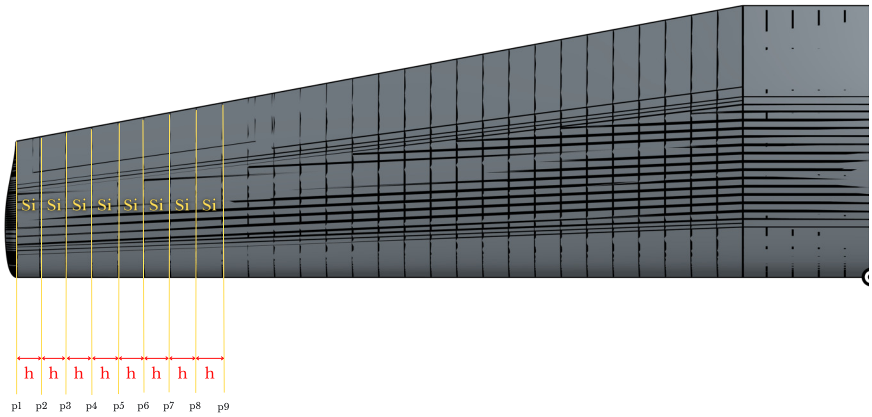

FIGURE 3.16: Baruna-1 Tapered Wing (Half Wing)

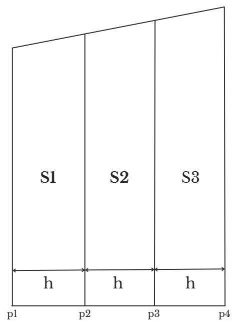

FIGURE 3.17: Tapered Wing Geometry

Since h_i is equal to the rib spacing and p_i is equal to the chord length, the area cross section of the wing can be calculated as follows:

$$S_i = \left(\frac{c_1 + c_2}{2}\right) \times (h) \tag{3.6}$$

The spars are subjected not only to torsional force but also to shear force along the span. Therefore, the shear flow on both front and rear spars must be determined using the equation:

$$q_f = \left[\frac{V}{2h_f}\right] + \left[\frac{T(c_i)}{2h_f}\right] \tag{3.7}$$

Where q_f is the shear flow at front spar (N/m), V is the shear load (N), and T is the torsion (N).

For the aft spar, the shear flow can be calculated by equation of:

$$q_r = \left[\frac{V}{2h_f}\right] - \left[\frac{T(c_i)}{2h_f}\right] \tag{3.8}$$

The shear flows between the front and rear spars must oppose each other to neutralize the shear force. Therefore, the equations of the two shear flows are slightly different [9].

Finally, the spar thickness can be calculated by substituting the shear flow acting on the spar structures. Therefore the formula becomes:

$$\begin{aligned} t_{fs} &= \left[\frac{q_f(h_f)}{8.1E}\right]^{\frac{1}{3}} \times 1000 \\ t_{rs} &= \left[\frac{q_r(h_r)}{8.1E}\right]^{\frac{1}{3}} \times 1000 \end{aligned} \tag{3.9}$$

Where the t_{fs} is the front spar thickness and t_{rs} is the rear spar thickness.

Ribs Thickness

Another important supporting substructure of the wing is the wing ribs [20]. The thickness of the ribs across the span ideally varies depending on the magnitude of the load acting on the wing span. In analyzing the rib thickness, the first step is to determine the parameters needed.

The equivalent panel thickness or defined as the average skin thickness on the area cross section of the wing stringers (as shown in Figure 3.18) [9].

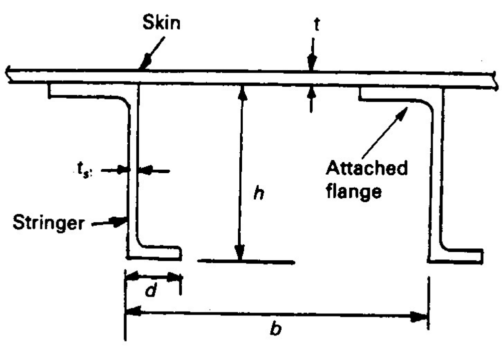

FIGURE 3.18: Skin-Stringer Section

The equivalent panel thickness can be determined by the formula of [9]:

$$T = \frac{t_{skin} + A_{stringer}}{b} \tag{3.10}$$

Where T is the equivalent panel thickness (mm), t_{skin} is the skin thickness, $A_{stringer}$ is the cross section area of stringer, and b is the stringer spacing.

Since the stringer specification data is not available on the report, the cross-section area of the stringer cannot be calculated. Hence, data are specified by using OnShape software.

Additionally, to calculate the rib thickness, the second moment of inertia of the skin panel, as well as the crush load need to be determined. Equation 3.10 shows how to calculate the skin panel second moment of inertia.

$$I_{skinpanel} = \frac{1}{12}\left[c_{wingbox}\left(\frac{T}{1000}\right)\right]^3 + \left[c_{wb}\left(\frac{h_{spar}}{2}\right)\right]^2 \tag{3.11}$$

Where c_{wb} is the wing box chord, and h_{spar} is the average spar height.

When the wing is subjected to bending, a curvature is created on the wing, resulting in a radial load. This reaction is called a crushing load which can be calculated by equation:

$$F = \frac{M^2 s h_{spar} t_e c_{wb}}{2EI^2} \tag{3.12}$$

Where F is the crush load, M is the bending moment, t_e is the equivalent panel thickness, and s is the rib spacing.

As the ribs are subjected to buckling the rib thickness can be determined by analyzing the yield of material and plate buckling which is shown in the equation of [9]:

$$\begin{gathered} \sigma_{yield,material} = \frac{F}{t_r c} = \sigma_{rib} \\ \sigma_{rib} = \sigma_{cr,buckling} = KE(\frac{t_r}{h_c})^2 \end{gathered} \tag{3.13}$$

Where F is the crushing load, t_r is the rib thickness, h_c is the spar height, and K is the compression coefficient (which is shown in Appendix A).

After performing some mathematical operations, the rib thickness can be obtained based on [9]:

$$t_r = \sqrt[3]{\frac{F(h_c)^2}{3.62Ec}} \tag{3.14}$$

CHAPTER 4
RESULTS AND DISCUSSIONS

In this chapter, the load distribution along the wing span are discussed along with the results of the dimension of skin thickness, rib, and spar, respectively. Detail calculation are shown in Appendices B, C, D. All the plots are represented for half wing span $b/2$ with length 20 m. The wing station range from $0 - 1$, where the value represents the nondimensional location of wing span $\frac{y}{b/2}$.

4.1 Wing Loading Distribution

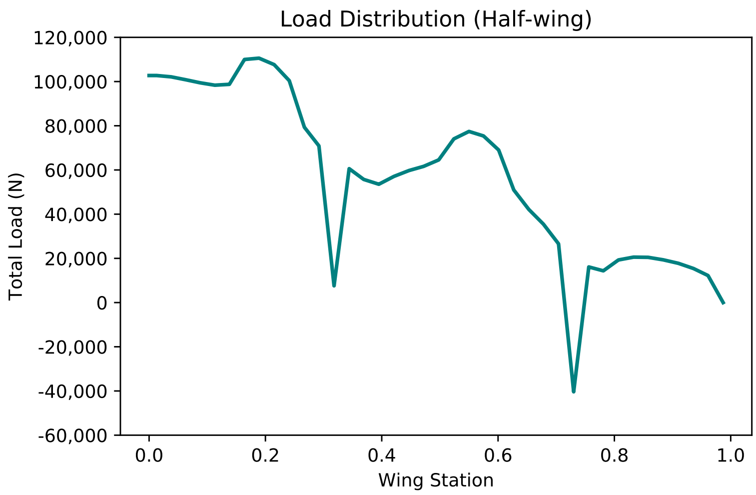

FIGURE 4.1: Half Span Load Distribution

Figure 4.1 shows the load distribution over half the wingspan. The load distribution is the total load including the ones contributed from the fuel and engines. The maximum fuel mass is considered as a distributed mass along the wing span. From this figure, the maximum load of ~ 110 kN is occurred at 0.2.

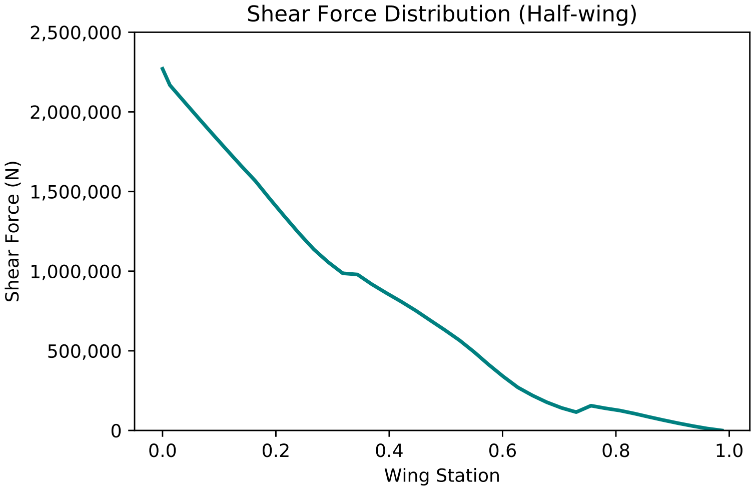

FIGURE 4.2: Shear Force Distribution

Figure 4.2 represented the shear force distribution along the half wingspan which shows that the magnitude of shear force acting on the wing root is 2270.488 kN. The maximum value is on the wing root which is reduced on the tip.

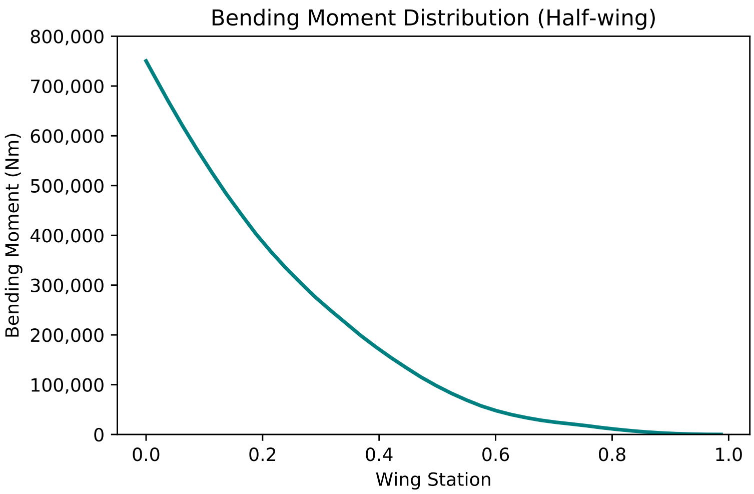

FIGURE 4.3: Bending Moment Distribution

Figure 4.3 represents the bending moment distribution along half the span, showing that the bending moment acting on the wing root is 750.324 kNm. Like that in the shear stress, the bending moment is also maximum at the wing root.

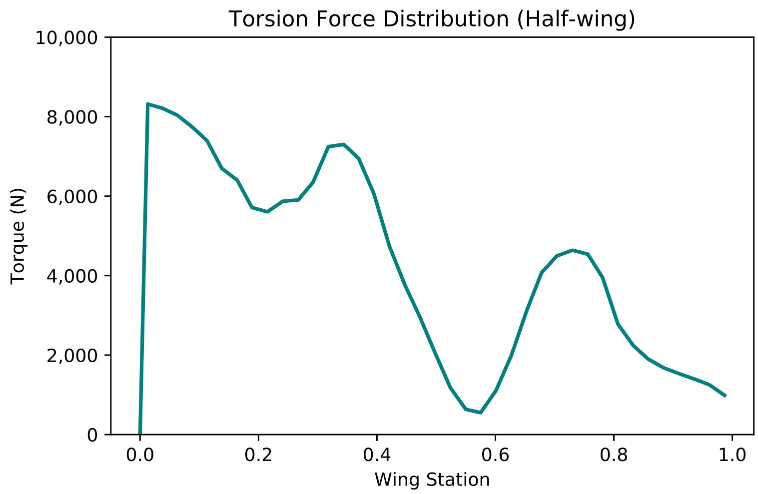

FIGURE 4.4: Torsion Force Distribution

The torsion force distributed along the half wing span of Baruna-1 is shown in Figure 4.4. According to the figure, the torsion at wing root is 0 N and 987.740 at the tip. The maximum torsion force is at the second wing station which is 8316.842 N.

4.2 Parametric Analysis of Wing Structural Components

In this section, the dimension of skin, rib, and spar along the wing span are shown and discuss.

4.2.1 Skin Thickness

After utilizing some calculation to the preliminary design of Baruna-1 wing, the skin thickness across the wing span is distributed as follows (shown in Figure 4.5). The torque originating from the aerodynamics moment is distributed along the skin. The figure shows that the skin thickness of the wing is not uniform along the span. It varies linearly along the span, that is 2.845 mm at root to 0.163 mm at the tip. This is in accordance to the load applied to the span, which concludes that the required skin thickness deviates parallel to the load acting on the wing span.

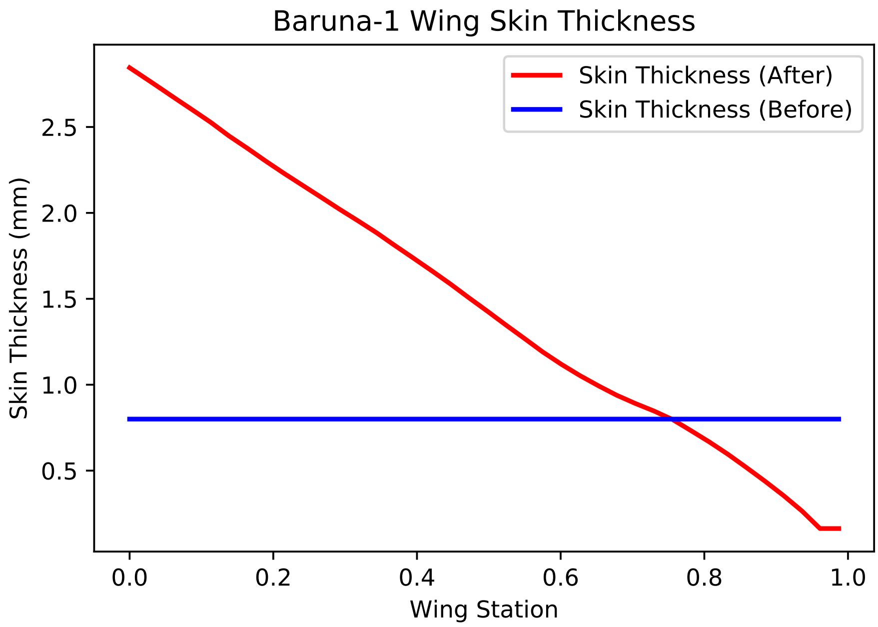

FIGURE 4.5: Wing Skin Thickness Result

4.2.2 Rib Thickness

The calculation result of the rib thickness also varies for each stations as shown in Figure 4.6. From the figure, it can be seen that the rib thickness at root and tip are 39.424 mm and 0 mm, respectively.

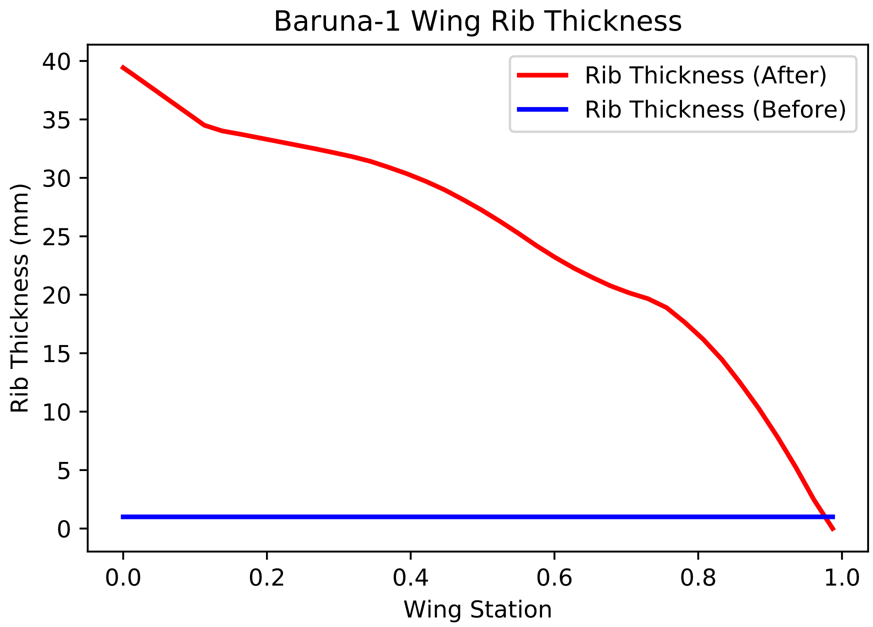

FIGURE 4.6: Wing Rib Thickness Result

According to the theory of elliptical lift distribution, the forces acting on the wing decrease toward the tip. Therefore, theoretically, the thickness of the ribs will be smaller the closer they get to the tip. The result shows that the required rib thickness decreases towards the tip, which means that the result is consistent with the mentioned theory. There are two particular *extrema* points that take place in the position of the engines. Based on the diagram, the line is approaching to zero, which means that no more ribs are needed at the last wing station.

4.2.3 Spar Thickness

The calculations on spar thickness were carried out by considering the load from the bending moment. From this analysis, the required thickness for both front and aft spars along the span are determined. Figure 4.7 shows the final result of the calculated thickness for front spars along the span which are 12.429 mm at wing root, and 1.065 mm at wing tip.

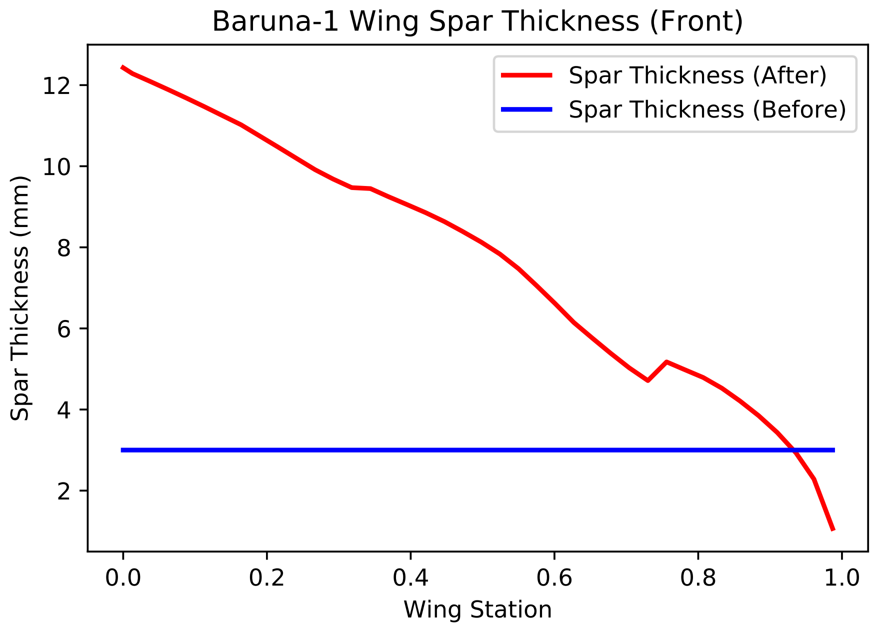

FIGURE 4.7: Front Spar Thickness Result

Additionally, Figure 4.8 shows the final result of the calculated thickness for aft spars along the span which are 12.429 mm at wing root, and 1.065 mm at wing tip. From this result, the dimenson of both spars are identical.

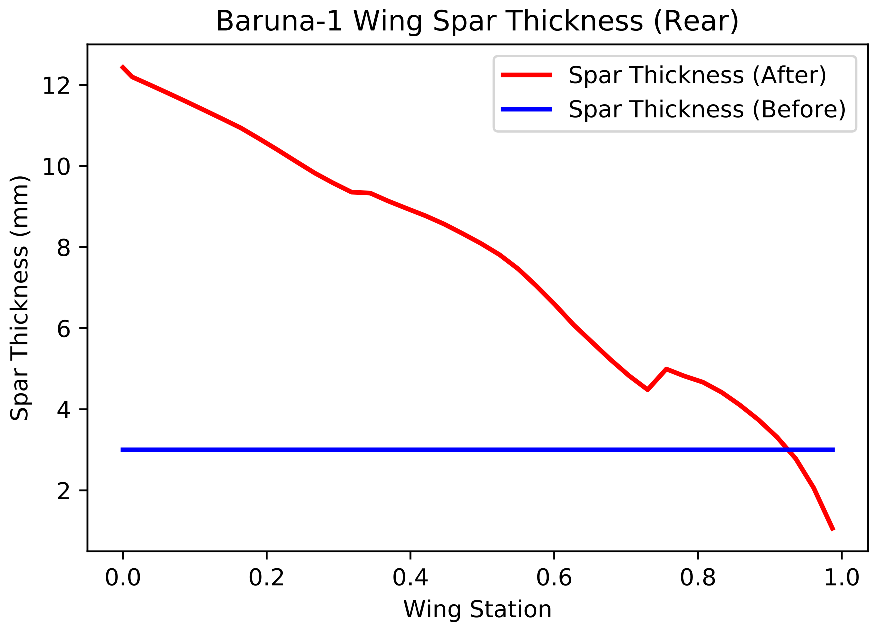

FIGURE 4.8: Aft Spar Thickness Result

Finally, just like the skin and rib thickness, the thickness of the spar also varies depending on the applied load across the span. The result indicates that the spar thickness for both the front and rear spars decreases further from the wing root. It also shows that at specific points where the load increases due to the engine placement, the required spar thickness also increases, resulting in extrema appearing in the lines.

CHAPTER 5
SUMMARY, CONCLUSION, RECOMMENDATION

5.1 Summary and Conclusion

Based on the parametric analysis of wing structural components for Baruna-1 aircraft with MTOM = 144 560 kg, it is concluded that:

- The required skin thickness of the wing varies across the span, ranging from 2.845 mm at wing root to 0.163 mm at wing tip.
- The required rib thickness varies depending on the wing station. The largest rib thickness is 39.42 mm which is the thickness at root, and the smallest rib thickness is 2.462 mm near the tip.
- The required spar thickness varies from 12.429 mm at wing root and 1.065 mm at wing tip for both front and rear spars.

In summary, the thickness of each main substructure is not uniform. At certain points in the span, the values are either lower or higher than the required size. This could definitely lead to a miscalculation of the aircraft weight. In addition, according to the V-n diagram of Baruna-1, the design have met the requirement stated by FAR 25.

5.2 Recommendation

The recommendations for the future work are as the following:

- Consider the dimension of skin, rib, and spar for zero fuel mass assumption.
- Perform the same analysis for the aircraft fuselage and empennage. By doing the structural analysis for the entire aircraft components, a more accurate weight analysis can be obtained.
- Consider performing some weight analysis with the new configuration to get the MTOM and new c.g of the aircraft.
- Based on the new design, analyze the stability and performance of Baruna-1 aircraft.

Bibliography

[1] "BARUNA 1: An Aerial Firefighting," en, p. 100,

[2] J. Roskam, *Airplane design*, eng. Lawrence, Kan: DARcorporation, 2002, ISBN: 978-1-884885-24-2.

[3] E. F. Bruhn, *Analysis and design of flight vehicle structures*, eng. Carmel, Ind: Jacobs Publ, 1973, ISBN: 978-0-9615234-0-4.

[4] D. Solano, D. Sarojini, J. A. Corman, and D. N. Mavris, "Structural Sizing of Unconventional Aircraft under Static and Dynamic Aeroelastic Loading," en, in *AIAA Scitech 2020 Forum*, Orlando, FL: American Institute of Aeronautics and Astronautics, Jan. 2020, ISBN: 978-1-62410-595-1. DOI: 10.2514/6.2020-0274. [Online]. Available: https://arc.aiaa.org/doi/10.2514/6.2020-0274 (visited on 09/09/2022).

[5] T. H. G. Megson, *Aircraft structures for engineering students* (Elsevier aerospace engineering series), 4th ed. Oxford ; Burlington, MA: Butterworth-Heinemann, 2007, OCLC: ocm76798397, ISBN: 978-0-7506-6739-5.

[6] S. Gudmundsson, *General aviation aircraft design: applied methods and procedures*, First edition. Oxford ; Waltham, MA: Butterworth-Heinemann, 2014, OCLC: ocn863648682, ISBN: 978-0-12-397308-5.

[7] M. H. Sadraey, *Aircraft design: a systems engineering approach* (Aerospace series). Chichestet, West Sussex: Wiley, 2013, ISBN: 978-1-119-95340-1.

[8] D. P. Raymer, *Aircraft design: a conceptual approach* (AIAA education series). Reston, VA: American Institute of Aeronautics and Astronautics, Inc, 2018, ISBN: 978-1-62410-490-9.

[9] M. C.-Y. Niu, *Airframe structural design: practical design information and data on aircraft structures*, eng, 2. ed., 3. publ. with minor corr. Hong Kong: Conmilit Press Ltd, 2006, ISBN: 978-962-7128-09-0.

[10] S. Nair, *Mechanics of aero-structures*. New York, NY: Cambridge University Press, 2015, ISBN: 978-1-107-07577-1.

[11] K. Arankumar, N. Lohith, and B. Ganesha, “Effect of Ribs and Stringer Spacing on the Weight of Aircraft Structure for Alumunium Material,” [Online]. Available: http://docsdrive.com/pdfs/ansinet/jas/2012/1006-1012.pdf.

[12] T. C. Corke, *Design of aircraft*. Upper Saddle River, N.J: Prentice Hall, 2003, ISBN: 978-0-13-089234-8.

[13] J. D. Anderson, *Fundamentals of aerodynamics* (McGraw-Hill series in aeronautical and aerospace engineering), Sixth edition. New York, NY: McGraw Hill Education, 2017, ISBN: 978-1-259-12991-9.

[14] T. M. Sunandar, “Conceptual & Preliminary Structural Design of a Regional Transport Aircraft for the Indonesian Market,” Individual Research Project, Sep. 2022.

[15] *FAR § 25.335*. [Online]. Available: https://www.govinfo.gov/content/pkg/CFR-2012-title14-vol1/pdf/CFR-2012-title14-vol1-sec25-335.pdf.

[16] *FAR § 25.337*. [Online]. Available: https://www.govinfo.gov/content/pkg/CFR-2012-title14-vol1/pdf/CFR-2012-title14-vol1-sec25-337.pdf.

[17] R. R. Craig, *Mechanics of materials*, 3rd ed. Hoboken, NJ: Wiley, 2011, ISBN: 978-0-470-48181-3.

[18] R. C. Hibbeler, *Mechanics of materials*, 8th ed. Boston: Prentice Hall, 2011, ISBN: 978-0-13-602230-5.

[19] F. P. Beer, Ed., *Statics and mechanics of materials* (Connect, learn, succeed), 1st ed. New York, NY: McGraw-Hill, 2011, ISBN: 978-0-07-338015-5.

[20] E. Torenbeek, *Advanced aircraft design: conceptual design, analysis, and optimization of subsonic civil airplanes*. Chichester, West Sussex, United Kingdom: John Wiley & Sons Inc, 2013, ISBN: 978-1-118-56809-5 978-1-118-56807-1 978-1-118-56808-8.

[21] T. L. Lomax, *Structural loads analysis for commercial transport aircraft: theory and practice* (AIAA education series). Reston, VA: American Institute of Aeronautics and Astronautics, 1996, ISBN: 978-1-56347-114-8.

[22] S. Gudmundsson, *General aviation aircraft design: applied methods and procedures*, eng, Second edition. Oxford Cambridge, MA: Butterworth-Heinemann, 2022, ISBN: 978-0-12-818465-3.

[23] *About ASM Aerospace Specification Metals, Inc.* [Online]. Available: https://www.aerospacemetals.com/asm-metal-distributor.html (visited on 05/13/2022).

[24] *Aerospace Aluminum Distributor Supplier*. [Online]. Available: https://www.aerospacemetals.com/aluminum-distributor.html (visited on 05/13/2022).

[25] J. Cutler and J. Liber, *Understanding aircraft structures*, 4th ed. Malden, MA: Blackwell Pub, 2005, ISBN: 978-1-4051-2032-6.

Appendices

APPENDIX A
COMPRESSION BUCKLING COEFFICIENT

This table consists of the reference data used in the calculation of rib thickness.

	Support conditions at edges	Sources							
		McDonnell-Douglas	Lockheed	NASA	Convair	Rockwell Int'l	Northrop	Republic	Boeing
Plate panel all edges supported	①	3.62	3.62	4.0	4.0	3.62	3.62	3.62	3.62
	②	6.3	6.3	6.98	6.98	6.98	6.28	6.45	6.3
	③	6.25	6.3	—	6.98	6.98	6.28	6.3	6.3
	④	3.7	6.32	—	4.0	4.0	3.62	3.7	6.32
	⑤	5.1	5.02	—	5.4	—	4.9	5.0	5.0
	⑥	5.0	5.02	—	5.4	5.41	4.9	4.9	5.0
Plate panel one edge free	⑦	1.2	1.16	1.28	1.28	—	1.2	1.05	1.12
	⑧	1.17	1.16	—	1.28	1.28	1.2	1.14	1.12
	⑨	0.45	0.378	—	0.429	—	0.367	0.4	0,4
	⑩	0.429	0.378	0.43	0.429	0.429	0.367	0.388	0.4

Simply supported edge *Fixed edge*

APPENDIX B
BARUNA-1 INERTIAL WING LOADING

WING INERTIAL LOAD										
Chord Length (c)	Max. Thickness	Area	Rib Thickness	Volume	Wing Mass	Wing Weight n=3.15	Shear Force	dM	Bending Moment	Wing Weight n=1
m	m	m2	m	m3	kg	N	N	Nm	Nm	N
6.35	1.0795	6.854825	0.001	0.006854825	688.4212854	-21273.25035	-548464.8522	-3427.905326	-108726.6942	-6753.41281
6.35	1.0795	6.854825	0.001	0.006854825	688.4212854	-21273.25035	-527191.6019	-6589.895023	-105298.7889	-6753.41281
6.35	1.0795	6.854825	0.001	0.006854825	688.4212854	-21273.25035	-505918.3515	-6323.979394	-98708.89384	-6753.41281
6.35	1.0795	6.854825	0.001	0.006854825	688.4212854	-21273.25035	-484645.1012	-6058.063765	-92384.91444	-6753.41281
6.35	1.0795	6.854825	0.001	0.006854825	688.4212854	-21273.25035	-463371.8508	-5792.148135	-86326.85068	-6753.41281
6.35	1.0795	6.854825	0.001	0.006854825	688.4212854	-21273.25035	-442098.6005	-5600.72612	-80534.70254	-6753.41281
6.299100342	1.070847058	6.74537307	0.001	0.006745373	677.4291684	-20933.57745	-420825.3501	-5415.391018	-74933.97642	-6645.580142
6.205572084	1.054947254	6.546551231	0.001	0.006546551	657.4617461	-20316.55415	-399891.7727	-5146.007277	-69518.5854	-6449.699729
6.112043826	1.03904745	6.350703554	0.001	0.006350704	637.793015	-19708.76085	-379575.2185	-4884.563699	-64372.57813	-6256.749477
6.018515568	1.023147647	6.157830039	0.001	0.00615783	618.4229752	-19110.19757	-359866.4577	-4630.94151	-59488.01443	-6066.729387
5.92498731	1.007247843	5.967930686	0.001	0.005967931	599.3516266	-18520.86429	-340756.2601	-4385.021933	-54857.07292	-5879.639457
5.831459052	0.991348039	5.781005495	0.001	0.005781005	580.5789694	-17940.76102	-322235.3958	-4146.686191	-50472.05099	-5695.479689
5.737930794	0.975448235	5.597054465	0.001	0.005597054	562.1050033	-17369.88776	-304294.6348	-3915.815508	-46325.36479	-5514.250083
5.644402536	0.959548431	5.416077598	0.001	0.005416078	543.9297286	-16808.24451	-286924.747	-3692.291107	-42409.54929	-5335.950638
5.550874278	0.943648627	5.238074893	0.001	0.005238075	526.0531451	-16255.83126	-270116.5025	-3475.994213	-38717.25818	-5160.581354
5.45734602	0.927748823	5.063046349	0.001	0.005063046	508.4752529	-15712.64803	-253860.6713	-3266.806048	-35241.26397	-4988.142231
5.363817762	0.91184902	4.890991967	0.001	0.004890992	491.196052	-15178.6948	-238148.0232	-3064.607837	-31974.45792	-4818.63327
5.270289504	0.895949216	4.721911748	0.001	0.004721912	474.2155423	-14653.97158	-222969.3284	-2869.22506	-28909.85008	-4652.05447
5.176763063	0.880049721	4.555808888	0.001	0.004555809	457.5340451	-14138.48829	-208315.3568	-2680.70617	-26040.62502	-4488.408982
5.083234805	0.864149917	4.392676934	0.001	0.004392677	441.1509121	-13632.22491	-194176.8685	-2498.765033	-23359.91885	-4327.690448
4.989706547	0.848250113	4.232519142	0.001	0.004232519	425.0664705	-13135.19154	-180544.6436	-2323.29361	-20861.15382	-4169.902075
4.896180106	0.832350618	4.075338537	0.001	0.004075339	409.2810238	-12647.39756	-167409.4521	-2154.308534	-18537.86021	-4015.046844
4.802651848	0.816450814	3.921129011	0.001	0.003921129	393.7939589	-12168.82402	-154762.0545	-1991.516808	-16383.55167	-3863.118737
4.709125407	0.800551319	3.769896557	0.001	0.003769897	378.6058774	-11699.48952	-142593.2305	-1834.960987	-14392.03487	-3714.123657
4.615597149	0.784651515	3.621635297	0.001	0.003621635	363.7161892	-11239.37582	-130893.741	-1684.373383	-12557.07388	-3568.055816
4.522070708	0.76875202	3.476350993	0.001	0.003476351	349.1254728	-10788.5008	-119654.3652	-1539.742285	-10872.7005	-3424.920888
4.428544267	0.752852525	3.334040735	0.001	0.003334041	334.8334361	-10346.85543	-108865.8644	-1400.913159	-9332.958212	-3284.716008
4.335017826	0.73695303	3.194704524	0.001	0.003194705	320.840079	-9914.439702	-98519.00896	-1267.791867	-7932.045053	-3147.441175
4.241489568	0.721053227	3.058339738	0.001	0.00305834	307.1451385	-9491.245497	-88604.56926	-1140.185748	-6664.253186	-3013.093809
4.147963127	0.705153732	2.924951678	0.001	0.002924952	293.7491466	-9077.289252	-79113.32376	-1018.03025	-5524.067438	-2881.679128
4.054438503	0.689254546	2.794540168	0.001	0.00279454	280.6520858	-8672.570431	-70036.03451	-901.241201	-4506.037187	-2753.196962
3.960912062	0.673355051	2.667100142	0.001	0.0026671	267.8534474	-8277.073306	-61363.46408	-789.6403966	-3604.795986	-2627.642319
3.867385621	0.657455556	2.542634162	0.001	0.002542634	255.3534887	-7890.805831	-53086.39077	-683.1156764	-2815.15559	-2505.017724
3.773860997	0.641556369	2.42114456	0.001	0.002421145	243.1524438	-7513.775241	-45195.58494	-581.5880859	-2132.039913	-2385.325473
3.680334556	0.625656875	2.302626615	0.001	0.002302627	231.2498385	-7145.966885	-37681.8097	-484.8895272	-1550.451828	-2268.560916
3.586809932	0.609757688	2.187084933	0.001	0.002187085	219.6461355	-6787.395057	-30535.84281	-392.9352253	-1065.5623	-2154.728589
3.493285308	0.593858502	2.074517181	0.001	0.002074517	208.3411005	-6438.052519	-23748.44776	-305.5950257	-672.627075	-2043.826196
3.399760684	0.577959316	1.96492336	0.001	0.001964923	197.3347336	-6097.939271	-17310.39524	-222.7501659	-367.0320493	-1935.853737
3.30623606	0.56206013	1.85830347	0.001	0.001858303	186.6270348	-5767.055315	-11212.45597	-144.2818834	-144.2818834	-1830.811211
3.212711436	0.546160944	1.754657511	0.001	0.001754658	176.218004	-5445.40065	0	0	0	-1728.698619

Fuel Weight Distribution										
Wing Station	Fuel	Fuel Weight	Shear Force	dM	Bending Moment	Wing Box Chord	Max c Thickness	Rib Thickness	Area	Volume
m	N/m	N	N	Nm	Nm	m	m	m	m2	m3
0	27814.0758	-18345.36343	-472978.359	-5797.570966	-179333.0655	2.8575	0.485775	0.001	1.388102063	0.001388102
0.0125	27814.0758	-18345.36343	-454632.9956	-11136.50785	-173535.4946	2.8575	0.485775	0.001	1.388102063	0.001388102
0.0375	27814.0758	-18345.36343	-436287.6321	-10677.87376	-162398.9867	2.8575	0.485775	0.001	1.388102063	0.001388102
0.0625	27814.0758	-18345.36343	-417942.2687	-10219.23968	-151721.113	2.8575	0.485775	0.001	1.388102063	0.001388102
0.0875	27814.0758	-18345.36343	-399596.9053	-9760.605589	-141501.8733	2.8575	0.485775	0.001	1.388102063	0.001388102
0.1125	27814.0758	-18345.36343	-381251.5419	-9427.362079	-131741.2677	2.8575	0.485775	0.001	1.388102063	0.001388102
0.137837	27814.0758	-18052.4405	-362906.1784	-9107.808484	-122313.9056	2.834595154	0.481881176	0.001	1.365938047	0.001365938
0.163574	27814.0758	-17520.33955	-344853.7379	-8650.040164	-113206.0971	2.792507438	0.474726264	0.001	1.325676624	0.001325677
0.189311	27814.0758	-16996.19826	-327333.3984	-8205.864097	-104556.057	2.750419722	0.467571353	0.001	1.28601747	0.001286017
0.215048	27814.0758	-16480.01663	-310337.2001	-7775.075426	-96350.19288	2.708332006	0.460416441	0.001	1.246960583	0.001246961
0.240785	27814.0758	-15971.79466	-293857.1835	-7357.469292	-88575.11746	2.66624429	0.453261529	0.001	1.208505964	0.001208506
0.266522	27814.0758	-15471.53236	-277885.3888	-6952.840838	-81217.64816	2.624156573	0.446106617	0.001	1.170653613	0.001170654
0.292259	27814.0758	-14979.22971	-262413.8565	-6560.985207	-74264.80732	2.582068857	0.438951706	0.001	1.133403529	0.001133404
0.317996	27814.0758	-14494.88672	-247434.6268	-6181.697539	-67703.82212	2.539981141	0.431796794	0.001	1.096755714	0.001096756
0.343733	27814.0758	-14018.5034	-232939.74	-5814.772979	-61522.12458	2.497893425	0.424641882	0.001	1.060710166	0.00106071
0.36947	27814.0758	-13550.07974	-218921.2366	-5460.006666	-55707.3516	2.455805709	0.417486971	0.001	1.025266886	0.001025267
0.395207	27814.0758	-13089.61573	-205371.1569	-5117.193745	-50247.34493	2.413717993	0.410332059	0.001	0.990425873	0.000990426
0.420944	27814.0758	-12637.11139	-192281.5412	-4786.036376	-45130.15119	2.371630277	0.403177147	0.001	0.956187129	0.000956187
0.4466805	27814.0758	-12192.57527	-179644.4298	-4466.608535	-40344.11481	2.329543378	0.396022374	0.001	0.9225513	0.000922551
0.4724175	27814.0758	-11755.99009	-167451.8545	-4158.426421	-35877.50628	2.287455662	0.388867463	0.001	0.889517079	0.000889517
0.4981545	27814.0758	-11327.36458	-155695.8644	-3861.303256	-31719.07986	2.245367946	0.381712551	0.001	0.857085126	0.000857085
0.523891	27814.0758	-10906.70682	-144368.4999	-3575.259124	-27857.7766	2.203281048	0.374557778	0.001	0.825256054	0.000825256
0.549628	27814.0758	-10494.00047	-133461.793	-3299.800015	-24282.51748	2.161193332	0.367402866	0.001	0.794028625	0.000794029
0.5753645	27814.0758	-10089.26157	-122967.7926	-3034.988415	-20982.71746	2.119106433	0.360248094	0.001	0.763404053	0.000763404
0.6011015	27814.0758	-9692.474386	-112878.531	-2780.37313	-17947.72905	2.077018717	0.353093182	0.001	0.733381148	0.000733381
0.626838	27814.0758	-9303.654341	-103186.0566	-2535.926196	-15167.35592	2.034931819	0.345938409	0.001	0.703961076	0.000703961
0.6525745	27814.0758	-8922.793649	-93882.40227	-2301.383707	-12631.42972	1.99284492	0.338783636	0.001	0.675143249	0.000675143
0.678311	27814.0758	-8549.892307	-84959.60862	-2076.581158	-10330.04602	1.950758022	0.331628864	0.001	0.646927666	0.000646928
0.704048	27814.0758	-8184.943305	-76409.71631	-1861.192767	-8253.464858	1.908670306	0.324473952	0.001	0.619313797	0.000619314
0.7297845	27814.0758	-7827.960821	-68224.77301	-1655.102558	-6392.272091	1.866583407	0.317319179	0.001	0.592302715	0.000592303
0.7555205	27814.0758	-7478.944392	-60396.81219	-1458.161631	-4737.169532	1.824497326	0.310164545	0.001	0.565894384	0.000565894
0.781257	27814.0758	-7137.880456	-52917.8678	-1270.068674	-3279.007901	1.782410428	0.303009773	0.001	0.540087779	0.000540088
0.8069935	27814.0758	-6804.775872	-45779.98734	-1090.629898	-2008.939227	1.740323529	0.295855	0.001	0.514883418	0.000514883
0.8327295	27814.0758	-6479.636879	-38975.21147	-919.7039427	-918.3093288	1.698237449	0.288700366	0.001	0.490281773	0.000490282
0.858466	27814.0758	-6162.450843	-32495.57459	-757.0076902	1.394613934	1.65615055	0.281545594	0.001	0.46628189	0.000466282
0.884202	27814.0758	-5853.230089	-26333.12375	-602.389908	758.4023041	1.614064469	0.27439096	0.001	0.442884699	0.000442885
0.909938	27814.0758	-5551.968377	-20479.89366	-455.6278141	1360.792212	1.571978389	0.267236326	0.001	0.420089729	0.00042009
0.935674	27814.0758	-5258.665707	-14927.92528	-316.5165747	1816.420026	1.529892308	0.260081692	0.001	0.39789698	0.000397897
0.96141	27814.0758	-4973.32208	-9669.259574	-184.8513559	2132.936601	1.487806227	0.252927059	0.001	0.376306453	0.000376306
0.987146	27814.0758	-4695.937494	-4695.937494	2317.787957	2317.787957	1.445720146	0.245772425	0.001	0.355318146	0.000355318

Powerplant Load Distribution					
Wing Station	Powerplant Weight	Shear Force	dM	Bending Moment	Poweplant Actual Weight n=3.15
m	N	N	Nm	Nm	N
0	0	-121133.88	-1514.1735	-65019.63973	0
0.0125	0	-121133.88	-3028.347	-63505.46623	0
0.0375	0	-121133.88	-3028.347	-60477.11923	0
0.0625	0	-121133.88	-3028.347	-57448.77223	0
0.0875	0	-121133.88	-3028.347	-54420.42523	0
0.1125	0	-121133.88	-3069.169118	-51392.07823	0
0.137837	0	-121133.88	-3117.62267	-48322.90911	0
0.163574	0	-121133.88	-3117.62267	-45205.28644	0
0.189311	0	-121133.88	-3117.62267	-42087.66377	0
0.215048	0	-121133.88	-3117.62267	-38970.0411	0
0.240785	0	-121133.88	-3117.62267	-35852.41843	0
0.266522	0	-121133.88	-3117.62267	-32734.79576	0
0.292259	0	-121133.88	-3117.62267	-29617.17309	0
0.317996	-60566.94	-121133.88	-2338.217002	-26499.55042	-190785.861
0.343733	0	-60566.94	-1558.811335	-24161.33342	0
0.36947	0	-60566.94	-1558.811335	-22602.52209	0
0.395207	0	-60566.94	-1558.811335	-21043.71075	0
0.420944	0	-60566.94	-1558.781051	-19484.89942	0
0.4466805	0	-60566.94	-1558.811335	-17926.11837	0
0.4724175	0	-60566.94	-1558.811335	-16367.30703	0
0.4981545	0	-60566.94	-1558.781051	-14808.4957	0
0.523891	0	-60566.94	-1558.811335	-13249.71464	0
0.549628	0	-60566.94	-1558.781051	-11690.90331	0
0.5753645	0	-60566.94	-1558.811335	-10132.12226	0
0.6011015	0	-60566.94	-1558.781051	-8573.310924	0
0.626838	0	-60566.94	-1558.781051	-7014.529873	0
0.6525745	0	-60566.94	-1558.781051	-5455.748821	0
0.678311	0	-60566.94	-1558.811335	-3896.96777	0
0.704048	0	-60566.94	-1558.781051	-2338.156435	0
0.7297845	-60566.94	-60566.94	-779.3753839	-779.3753839	-190785.861
0.7555205	0	0	0	0	0
0.781257	0	0	0	0	0
0.8069935	0	0	0	0	0
0.8327295	0	0	0	0	0
0.858466	0	0	0	0	0
0.884202	0	0	0	0	0
0.909938	0	0	0	0	0
0.935674	0	0	0	0	0
0.96141	0	0	0	0	0
0.987146	0	0	0	0	0

APPENDIX C
BARUNA-1 AERODYNAMIC WING LOADING

WING AERODYNAMIC LOADING								
Wing Station	Chord Length	Cl (airfoil)	dL	Lift	Shear Force	dM	Bending Moment	Lift (n=3.15)
m	-	-	N/m	N	N	Nm	Nm	N
0	6.35	0.32527	137.0648115	45190.53016	1080293.354	13221.22611	380198.8776	142350.17
0.0125	6.35	0.32527	137.0647848	45190.53016	1035102.824	25312.68897	366977.6515	142350.17
0.0375	6.35	0.32389	137.0645708	44998.8035	989912.2937	24185.3223	341664.9625	141746.231
0.0625	6.35	0.3209	137.0641429	44583.39573	944913.4902	23065.54481	317479.6402	140437.6965
0.0875	6.35	0.31772	137.0635011	44141.59081	900330.0945	21956.48248	294414.0954	139046.011
0.1125	6.35	0.31527	137.0626453	43801.20652	856188.5037	21138.35253	272457.6129	137973.8005
0.137837	6.299100342	0.31726	137.0615596	43724.3687	812387.2971	20345.74483	251319.2604	137731.7614
0.163574	6.205572084	0.34565	137.0602318	46929.73343	768662.9284	19179.16251	230973.5156	147828.6603
0.189311	6.112043826	0.34966	137.0586773	46758.66619	721733.195	17973.53334	211794.3531	147289.7985
0.215048	6.018515568	0.34537	137.0568959	45478.24534	674974.5288	16786.58265	193820.8197	143256.4728
0.240785	5.92498731	0.33037	137.0548878	42827.00747	629496.2835	15650.2265	177034.2371	134905.0735
0.266522	5.831459052	0.28052	137.0526528	35790.74694	586669.276	14638.53393	161384.0106	112740.8528
0.292259	5.737930794	0.26108	137.0501911	32776.20077	550878.5291	13756.18016	146745.4766	103245.0324
0.317996	5.644402536	0.25565	137.0475025	31571.37355	518102.3283	12928.1234	132989.2965	99449.82667
0.343733	5.550874278	0.23751	137.0445871	28845.16265	486530.9547	12150.65321	120061.1731	90862.26234
0.36947	5.45734602	0.22595	137.0414449	26978.85649	457685.7921	11432.28182	107910.5199	84983.39793
0.395207	5.363817762	0.2213	137.0380757	25970.78814	430706.9356	10750.89931	96478.23805	81807.98263
0.420944	5.270289504	0.23231	137.0344797	26787.49349	404736.1475	10071.7837	85727.33874	84380.60448
0.4466805	5.176763063	0.24129	137.0306569	27329.22479	377948.654	9375.578378	75655.55504	86087.05809
0.4724175	5.083234805	0.24837	137.0266071	27622.88337	350619.4292	8668.427175	66279.97666	87012.08263
0.4981545	4.989706547	0.25887	137.0223303	28260.92873	322996.5458	7949.131905	57611.54949	89021.92551
0.523891	4.896180106	0.2893	137.0178267	30990.995	294735.6171	7186.802958	49662.41758	97621.63425
0.549628	4.802651848	0.3024	137.013096	31775.51465	263744.6221	6378.9682	42475.61462	100092.8711
0.5753645	4.709125407	0.29942	137.0081383	30849.68711	231969.1074	5573.19972	36096.64642	97176.51438
0.6011015	4.615597149	0.28282	137.0029536	28560.62558	201119.4203	4808.584691	30523.4467	89965.97056
0.626838	4.522070708	0.228	136.9975419	22558.06778	172558.7948	4150.776566	25714.86201	71057.91349
0.6525745	4.428544267	0.20109	136.9919032	19484.1366	150000.727	3609.766969	21564.08545	61375.03029
0.678311	4.335017826	0.18056	136.9860373	17125.45564	130516.5904	3138.726561	17954.31848	53945.18526
0.704048	4.241489568	0.1514	136.9799442	14049.92415	113391.1347	2737.493003	14815.59192	44257.26108
0.7297845	4.147963127	0.12978	136.973624	11778.02192	99341.21059	2405.08581	12078.09891	37100.76905
0.7555205	4.054438503	0.11549	136.9670768	10244.83104	87563.18867	2121.736958	9673.013105	32271.21777
0.781257	3.960912062	0.10909	136.9603022	9453.874738	77318.35763	1868.249088	7551.276147	29779.70542
0.8069935	3.867385621	0.12748	136.9533003	10786.71575	67864.48289	1607.756873	5683.027059	33978.15461
0.8327295	3.773860997	0.13285	136.9460713	10969.25569	57077.76714	1327.82683	4075.270186	34553.15542
0.858466	3.680334556	0.13317	136.9386149	10723.17517	46108.51145	1048.662833	2747.443356	33778.00179
0.884202	3.586809932	0.12935	136.9309312	10150.8988	35385.33628	780.0552488	1698.780524	31975.33122
0.909938	3.493285308	0.12358	136.9230201	9445.217206	25234.43748	527.8924281	918.7252747	29752.4342
0.935674	3.399760684	0.11424	136.9148816	8497.599198	15789.22028	297.0042666	390.8328466	26767.43747
0.96141	3.30623606	0.1008	136.9065155	7291.621079	7291.621079	93.82858005	93.82858005	22968.6064
0.987146	3.212711436	0.07723	0	0	0	0	0	0

APPENDIX D
BARUNA-1 WING STRUCTURAL COMPONENTS FULL SPECIFICATION

BARUNA-1 DETAILED WING SKIN SPECIFICATION										
Wing Station	Area	Volume	Max. c Thickness (12%)	Combined Bending Moment	Combined Shear Force	Compressive Load	E (Young's Modulus) of AL2024	Stringer Spacing (report)	Skin Thickness	Skin Thickness (before)
m	m2	m3	m	Nm	N	N	Pa	m	mm	mm
0	6.854825	0.006855	1.0795	750324.9504	2270488.312	261924.4578	73000000000	0.1524	2.84471122	0.8
0.0125	6.854825	0.006855	1.0795	722585.9188	2167756.756	252241.2787	73000000000	0.1524	2.80921441	0.8
0.0375	6.854825	0.006855	1.0795	669676.1443	2065025.2	233771.4625	73000000000	0.1524	2.73890309	0.8
0.0625	6.854825	0.006855	1.0795	619327.1096	1962897.582	216195.5527	73000000000	0.1524	2.66846649	0.8
0.0875	6.854825	0.006855	1.0795	571514.9085	1862078.5	199505.2043	73000000000	0.1524	2.59795073	0.8
0.1125	6.854825	0.006855	1.0795	526205.7885	1762651.102	183688.6348	73000000000	0.1524	2.52739776	0.8
0.137837	6.745373	0.006745	1.0708471	482791.5102	1664295.916	167170.21	73000000000	0.1524	2.44924632	0.8
0.163574	6.546551	0.006547	1.0549473	441228.2358	1565550.172	152553.1699	73000000000	0.1524	2.37567255	0.8
0.189311	6.350704	0.006351	1.0390475	402351.1001	1455558.406	138899.6619	73000000000	0.1524	2.30257206	0.8
0.215048	6.15783	0.006158	1.0231476	366312.4544	1344973.566	126259.5116	73000000000	0.1524	2.23049302	0.8
0.240785	5.967931	0.005968	1.0072478	333082.373	1237307.307	114619.3087	73000000000	0.1524	2.15972653	0.8
0.266522	5.781005	0.005781	0.991348	302529.952	1136894.893	103930.8228	73000000000	0.1524	2.09039146	0.8
0.292259	5.597054	0.005597	0.9754482	274290.5277	1057566.333	94065.75722	73000000000	0.1524	2.02204129	0.8
0.317996	5.416078	0.005416	0.9595484	247984.267	986670.4185	84891.30754	73000000000	0.1524	1.95404207	0.8
0.343733	5.238075	0.005238	0.9436486	222687.8706	979090.663	76089.75452	73000000000	0.1524	1.8840318	0.8
0.36947	5.063046	0.005063	0.9277488	198268.6899	918502.7354	67615.29514	73000000000	0.1524	1.81131709	0.8
0.395207	4.890992	0.004891	0.911849	175346.2265	862782.0652	59678.44026	73000000000	0.1524	1.73747537	0.8
0.420944	4.721912	0.004722	0.8959492	153829.7797	809242.3931	52246.71349	73000000000	0.1524	1.66213321	0.8
0.446681	4.555809	0.004556	0.8800497	133737.3551	752152.8716	45324.60861	73000000000	0.1524	1.58522479	0.8
0.472418	4.392677	0.004393	0.8641499	115148.1667	692396.877	38937.19489	73000000000	0.1524	1.50695768	0.8
0.498155	4.232519	0.004233	0.8482501	98120.95498	630773.0094	33102.20204	73000000000	0.1524	1.42757345	0.8
0.523891	4.075339	0.004075	0.8323506	82717.83153	566213.64	27838.15172	73000000000	0.1524	1.34749233	0.8
0.549628	3.921129	0.003921	0.8164508	69098.32909	492146.1101	23195.90618	73000000000	0.1524	1.2679923	0.8
0.575365	3.769897	0.00377	0.8005513	57428.59992	414716.0635	19227.72307	73000000000	0.1524	1.19111983	0.8
0.601102	3.621635	0.003622	0.7846515	47725.18003	339328.3002	15935.05734	73000000000	0.1524	1.11882985	0.8
0.626838	3.476351	0.003476	0.768752	39880.40555	270294.1798	13277.58233	73000000000	0.1524	1.05281606	0.8
0.652575	3.334041	0.003334	0.7528525	33579.81951	219328.4215	11146.402	73000000000	0.1524	0.99317185	0.8
0.678311	3.194705	0.003195	0.736953	28476.89616	177223.0403	9422.919844	73000000000	0.1524	0.9390917	0.8
0.704048	3.05834	0.003058	0.7210532	24372.29214	141742.187	8038.24414	73000000000	0.1524	0.89063529	0.8
0.729785	2.924952	0.002925	0.7051537	21066.39622	115161.1147	6924.005663	73000000000	0.1524	0.84741986	0.8
0.755521	2.79454	0.002795	0.6892545	17583.11033	155532.5358	5758.248187	73000000000	0.1524	0.79691064	0.8
0.781257	2.6671	0.002667	0.6733551	13787.67959	139412.8328	4498.142266	73000000000	0.1524	0.73393438	0.8
0.806994	2.542634	0.002543	0.6574556	10384.53043	125048.0811	3374.344977	73000000000	0.1524	0.66687227	0.8
0.83273	2.421145	0.002421	0.6415564	7414.421164	105765.5082	2399.08997	73000000000	0.1524	0.5951983	0.8
0.858466	2.302627	0.002303	0.6256569	4956.955078	85205.76494	1596.79658	73000000000	0.1524	0.51967206	0.8
0.884202	2.187085	0.002187	0.6097577	3027.50212	64736.18088	970.675197	73000000000	0.1524	0.44022106	0.8
0.909938	2.074517	0.002075	0.5938585	1610.250766	45401.4748	513.7098354	73000000000	0.1524	0.35608373	0.8
0.935674	1.964923	0.001965	0.5779593	670.365145	27639.0615	212.7354169	73000000000	0.1524	0.26541539	0.8
0.96141	1.858303	0.001858	0.5620601	157.3528508	12228.22901	49.65509764	73000000000	0.1524	0.16341833	0.8
0.987146	1.754658	0.001755	0.5461609	0	0	0	73000000000	0.1524	0.16341833	0.8

BARUNA-1 DETAILED WING SPAR SPECIFICATION																
Chord Length (c)	Si (area section)	V_cruise	Rho_cruise	cm (moment coeff. per unit span)	Ribs Spacing	Torque	Shear Force (Comb.)	Wingbox Chord	Front Spar Height	Aft Spar Height	q_f (shear flow front spar)	q_r (shear flow rear spar)	t_f (front spar thickness)	t_r (rear spar thickness)	E (Young's Modulus) AL2024	Spar Thickness (Uniform) from report
m	m2	m/s	kg/m3	-	m	N	N	m	m	m	N/m	N/m	mm	mm	Pa	mm
6.35	0	151	0.6601	0.04568	0.6	0	2270488	2.8575	1.116	0.879	1017243.867	1291517.811	12.42874083	12.4287408	7.3E+10	3
6.35	3.81	151	0.6601	0.04568	0.6	8316.841557	2167757	2.8575	1.116	0.879	981864.7539	1219562.788	12.28294938	12.1935001	7.3E+10	3
6.35	3.81	151	0.6601	0.04509	0.6	8209.421756	2065025	2.8575	1.116	0.879	935700.5476	1161300.783	12.08734913	11.9961505	7.3E+10	3
6.35	3.81	151	0.6601	0.04413	0.6	8034.636995	1962898	2.8575	1.116	0.879	889720.6799	1103491.813	11.88602575	11.7936989	7.3E+10	3
6.35	3.81	151	0.6601	0.04251	0.6	7739.68771	1862078	2.8575	1.116	0.879	844173.2335	1046622.493	11.67963572	11.5875162	7.3E+10	3
6.35	3.81	151	0.6601	0.04063	0.6	7397.400886	1762651	2.8575	1.116	0.879	799188.6986	990621.7459	11.46837494	11.3770487	7.3E+10	3
6.29910034	3.79473	151	0.6601	0.03723	0.6	6697.089253	1664296	2.83459515	1.098	0.865	766520.6978	951047.6178	11.24879794	11.1635802	7.3E+10	3
6.20557208	3.751402	151	0.6601	0.03654	0.6	6401.438442	1565550	2.79250744	1.08	0.851	733067.7021	909326.7378	11.02182017	10.9382341	7.3E+10	3
6.11204383	3.695285	151	0.6601	0.03361	0.6	5712.635524	1455558	2.75041972	1.062	0.837	692688.5833	860123.2139	10.75519336	10.6780697	7.3E+10	3
6.01851557	3.639168	151	0.6601	0.03401	0.6	5605.724308	1344974	2.70833201	1.044	0.823	651415.5789	807892.7118	10.47732109	10.3987678	7.3E+10	3
5.92498731	3.583051	151	0.6601	0.03675	0.6	5871.260811	1237307	2.66624429	1.026	0.809	610605.0308	755038.9938	10.19451619	10.108887	7.3E+10	3
5.83145905	3.526934	151	0.6601	0.03814	0.6	5903.218689	1136895	2.62415657	1.008	0.795	571619.9717	705285.486	9.914101231	9.8244459	7.3E+10	3
5.73793079	3.470817	151	0.6601	0.04235	0.6	6347.081316	1057566	2.58206886	0.99	0.781	542401.482	666567.0502	9.683879894	9.58434266	7.3E+10	3
5.64440254	3.4147	151	0.6601	0.04995	0.6	7245.021139	986670.4	2.53998114	0.972	0.767	517012.6726	631204.8249	9.472250864	9.3551897	7.3E+10	3
5.55087428	3.358583	151	0.6601	0.05203	0.6	7299.698785	979090.7	2.49789343	0.954	0.753	522706.7781	638019.1191	9.447847526	9.33125942	7.3E+10	3
5.45734602	3.302466	151	0.6601	0.05125	0.6	6951.00113	918502.7	2.45580571	0.936	0.739	499771.925	609900.1537	9.248684014	9.13478719	7.3E+10	3
5.36381776	3.246349	151	0.6601	0.04619	0.6	6052.723473	862782.1	2.41371799	0.918	0.725	477882.1529	584946.5501	9.052847502	8.95121737	7.3E+10	3
5.2702895	3.190232	151	0.6601	0.03747	0.6	4741.04512	809242.4	2.37163028	0.9	0.711	455825.7774	561180.3002	8.852742605	8.77111314	7.3E+10	3
5.17676306	3.134116	151	0.6601	0.03088	0.6	3770.372387	752152.9	2.32954338	0.882	0.697	431369.6812	533263.7199	8.633166322	8.56621517	7.3E+10	3
5.08323481	3.077999	151	0.6601	0.02526	0.6	2974.2377	692396.9	2.28745566	0.864	0.683	404629.8113	501898.5653	8.393077758	8.33827587	7.3E+10	3
4.98970655	3.021882	151	0.6601	0.01815	0.6	2059.504883	630773	2.24536795	0.846	0.669	375530.352	467973.5898	8.129599973	8.08996286	7.3E+10	3
4.89618011	2.965766	151	0.6601	0.01078	0.6	1178.003712	566213.6	2.20328105	0.828	0.655	343483.7641	430242.8754	7.835070172	7.81116304	7.3E+10	3
4.80265185	2.90965	151	0.6601	0.00604	0.6	635.1734913	492146.1	2.16119333	0.81	0.641	304641.261	382818.5471	7.472890549	7.45900744	7.3E+10	3
4.70912541	2.853533	151	0.6601	0.00545	0.6	551.1290665	414716.1	2.11910643	0.792	0.627	262553.008	329783.2236	7.058483984	7.04524456	7.3E+10	3
4.61559715	2.797417	151	0.6601	0.01141	0.6	1108.675234	339328.3	2.07701872	0.774	0.613	220691.8859	274898.5	6.610583813	6.58074388	7.3E+10	3
4.52207071	2.7413	151	0.6601	0.02139	0.6	1995.438686	270294.2	2.03493182	0.756	0.599	181451.5618	222231.718	6.144570655	6.08333401	7.3E+10	3
4.42854427	2.685184	151	0.6601	0.03494	0.6	3126.73916	219328.4	1.99284492	0.738	0.585	152818.1082	182134.4575	5.75626926	5.64824294	7.3E+10	3
4.33501783	2.629069	151	0.6601	0.04751	0.6	4074.848556	177223	1.95075802	0.72	0.571	128591.7248	148225.9166	5.38988145	5.23099283	7.3E+10	3
4.24148957	2.572952	151	0.6601	0.05477	0.6	4498.072974	141742.2	1.90867031	0.702	0.557	107070.887	119530.3848	5.028057218	4.82882957	7.3E+10	3
4.14796313	2.516836	151	0.6601	0.05903	0.6	4637.630956	115161.1	1.86658341	0.684	0.543	90509.97056	98070.52463	4.71318929	4.48239525	7.3E+10	3
4.0544385	2.46072	151	0.6601	0.06047	0.6	4540.112382	155532.5	1.82449733	0.666	0.529	122984.9539	139176.8552	5.174155117	4.99349866	7.3E+10	3
3.96091206	2.404605	151	0.6601	0.05511	0.6	3950.053881	139412.8	1.78241043	0.648	0.515	113004.2053	128516.7142	4.98448826	4.81932618	7.3E+10	3
3.86738562	2.348489	151	0.6601	0.0406	0.6	2775.017525	125048.1	1.74032353	0.63	0.501	103077.3884	119978.6955	4.788858731	4.66707372	7.3E+10	3
3.773861	2.292374	151	0.6601	0.03436	0.6	2236.959688	105765.5	1.69823745	0.612	0.487	89513.39621	104688.5211	4.524916048	4.41780676	7.3E+10	3
3.68033456	2.236259	151	0.6601	0.03067	0.6	1899.576305	85205.76	1.65615055	0.594	0.473	74370.15933	86743.95412	4.211716136	4.10926509	7.3E+10	3
3.58680993	2.180143	151	0.6601	0.02855	0.6	1680.092363	64736.18	1.61406447	0.576	0.459	58548.57489	67564.70969	3.849257615	3.74318743	7.3E+10	3
3.49328531	2.124029	151	0.6601	0.02746	0.6	1533.305087	45401.47	1.57197839	0.558	0.445	42842.11224	48304.66556	3.432145822	3.312687	7.3E+10	3
3.39976068	2.067914	151	0.6601	0.02641	0.6	1397.277967	27639.06	1.52989231	0.54	0.431	27571.0614	29583.96367	2.930981803	2.78339761	7.3E+10	3
3.30623606	2.011799	151	0.6601	0.02508	0.6	1255.392747	12228.23	1.48780623	0.522	0.417	13501.92543	12422.59935	2.284298089	2.06148519	7.3E+10	3
3.21271144	1.955684	151	0.6601	0.02089	0.6	987.7397436	0	1.44572015	0.504	0.403	1416.661951	-1771.706261	1.064869273	1.06486927	7.3E+10	3

BARUNA-1 DETAILED WING RIB SPECIFICATION											
Skin Thickness	Stringer Area	Stringer Spacing	Eq. Panel Thickness	Spar Height (average)	Skin Panel 2nd Moment of Inertia (I_sp)	Bending Moment (n=3.15)	E_AL2024	Ribs Spacing	Crush Load	Rib Thickness (t_rib)	Rib Thickness (Preliminary Design)
mm	mm2	m	mm	m		Nm	Pa	m		mm	mm
2.844711	60.975	0.1524	3.24480964	0.9975	2.14518E-05	750324.9504	7.3E+10	0.6	4.65006E+07	3.94235E+01	1
2.809214	60.975	0.1524	3.20931284	0.9975	2.09843E-05	722585.9188	7.3E+10	0.6	4.45758E+07	3.88719E+01	1
2.738903	60.975	0.1524	3.13900151	0.9975	2.00736E-05	669676.1443	7.3E+10	0.6	4.09232E+07	3.77798E+01	1
2.668466	60.975	0.1524	3.06856491	0.9975	1.91815E-05	619327.1096	7.3E+10	0.6	3.74721E+07	3.66864E+01	1
2.597951	60.975	0.1524	2.99804916	0.9975	1.83088E-05	571514.9085	7.3E+10	0.6	3.42193E+07	3.55926E+01	1
2.527398	60.975	0.1524	2.92749619	0.9975	1.74561E-05	526205.7885	7.3E+10	0.6	3.11611E+07	3.44990E+01	1
2.449246	60.975	0.1524	2.84934474	0.9815	1.57545E-05	482791.5102	7.3E+10	0.6	3.05939E+07	3.40119E+01	1
2.375673	60.975	0.1524	2.77577098	0.9655	1.40411E-05	441228.2358	7.3E+10	0.6	3.03704E+07	3.37269E+01	1
2.302572	60.975	0.1524	2.70267049	0.9495	1.24884E-05	402351.1001	7.3E+10	0.6	3.01081E+07	3.34257E+01	1
2.230493	60.975	0.1524	2.63059145	0.9335	1.10882E-05	366312.4544	7.3E+10	0.6	2.98297E+07	3.31168E+01	1
2.159727	60.975	0.1524	2.55982495	0.9175	9.82980E-06	333082.373	7.3E+10	0.6	2.95480E+07	3.28047E+01	1
2.090391	60.975	0.1524	2.49048989	0.9015	8.70128E-06	302529.952	7.3E+10	0.6	2.92691E+07	3.24918E+01	1
2.022041	60.975	0.1524	2.42213972	0.8855	7.68784E-06	274290.5277	7.3E+10	0.6	2.89712E+07	3.21698E+01	1
1.954042	60.975	0.1524	2.35414049	0.8695	6.77561E-06	247984.267	7.3E+10	0.6	2.86208E+07	3.18263E+01	1
1.884032	60.975	0.1524	2.28413022	0.8535	5.94387E-06	222687.8706	7.3E+10	0.6	2.80900E+07	3.14136E+01	1
1.811317	60.975	0.1524	2.21141551	0.8375	5.18511E-06	198268.6899	7.3E+10	0.6	2.73300E+07	3.09121E+01	1
1.737475	60.975	0.1524	2.13757379	0.8215	4.50273E-06	175346.2265	7.3E+10	0.6	2.64153E+07	3.03471E+01	1
1.662133	60.975	0.1524	2.06223163	0.8055	3.88982E-06	153829.7797	7.3E+10	0.6	2.53203E+07	2.97058E+01	1
1.585225	60.975	0.1524	1.98532322	0.7895	3.34134E-06	133737.3551	7.3E+10	0.6	2.40390E+07	2.89805E+01	1
1.506958	60.975	0.1524	1.9070561	0.7735	2.85330E-06	115148.1667	7.3E+10	0.6	2.25837E+07	2.81694E+01	1
1.427573	60.975	0.1524	1.82767188	0.7575	2.42165E-06	98120.95498	7.3E+10	0.6	2.09734E+07	2.72712E+01	1
1.347492	60.975	0.1524	1.74759075	0.7415	2.04265E-06	82717.83153	7.3E+10	0.6	1.92411E+07	2.62896E+01	1
1.267992	60.975	0.1524	1.66809072	0.7255	1.71408E-06	69098.32909	7.3E+10	0.6	1.74671E+07	2.52497E+01	1
1.19112	60.975	0.1524	1.59121825	0.7095	1.43410E-06	57428.59992	7.3E+10	0.6	1.57664E+07	2.42001E+01	1
1.11883	60.975	0.1524	1.51892828	0.6935	1.19932E-06	47725.18003	7.3E+10	0.6	1.42378E+07	2.31929E+01	1
1.052816	60.975	0.1524	1.45291449	0.6775	1.00524E-06	39880.40555	7.3E+10	0.6	1.29562E+07	2.22795E+01	1
0.993172	60.975	0.1524	1.39327028	0.6615	8.45152E-07	33579.81951	7.3E+10	0.6	1.19158E+07	2.14730E+01	1
0.939092	60.975	0.1524	1.33919012	0.6455	7.12411E-07	28476.89616	7.3E+10	0.6	1.10730E+07	2.07622E+01	1
0.890635	60.975	0.1524	1.29073371	0.6295	6.02512E-07	24372.29214	7.3E+10	0.6	1.04285E+07	2.01597E+01	1
0.84742	60.975	0.1524	1.24751829	0.6135	5.11273E-07	21066.39622	7.3E+10	0.6	9.96742E+06	1.96658E+01	1
0.796911	60.975	0.1524	1.19700907	0.5975	4.26562E-07	17583.11033	7.3E+10	0.6	9.11181E+06	1.88959E+01	1
0.733934	60.975	0.1524	1.1340328	0.5815	3.46075E-07	13787.67959	7.3E+10	0.6	7.66695E+06	1.76561E+01	1
0.666872	60.975	0.1524	1.0669707	0.5655	2.76191E-07	10384.53043	7.3E+10	0.6	6.10053E+06	1.61879E+01	1
0.595198	60.975	0.1524	0.99529672	0.5495	2.16066E-07	7414.421164	7.3E+10	0.6	4.49467E+06	1.44611E+01	1
0.519672	60.975	0.1524	0.91977048	0.5335	1.65402E-07	4956.955078	7.3E+10	0.6	2.99957E+06	1.24949E+01	1
0.440221	60.975	0.1524	0.84031948	0.5175	1.23374E-07	3027.50212	7.3E+10	0.6	1.73698E+06	1.02933E+01	1
0.356084	60.975	0.1524	0.75618215	0.5015	8.89839E-08	1610.250766	7.3E+10	0.6	8.02244E+05	7.86062E+00	1
0.265415	60.975	0.1524	0.66551381	0.4855	6.11757E-08	670.365145	7.3E+10	0.6	2.43933E+05	5.21978E+00	1
0.163418	60.975	0.1524	0.56351676	0.4695	3.87854E-08	157.3528508	7.3E+10	0.6	2.66257E+04	2.46225E+00	1
0.163418	60.975	0.1524	0.56351676	0.4535	3.41704E-08	0	7.3E+10	0.6	0.00000E+00	0.00000E+00	1

Turnitin Report

AIRCRAFT STRUCTURAL WING ANALYSIS OF BARUNA-1

ORIGINALITY REPORT

16%	8%	9%	8%
SIMILARITY INDEX	INTERNET SOURCES	PUBLICATIONS	STUDENT PAPERS

PRIMARY SOURCES

1	www.ecfr.gov Internet Source	3%
2	Snorri Gudmundsson. "Aircraft Weight Analysis", Elsevier BV, 2022 Publication	2%
3	Megson, T.H.G.. "Bending of Open and Closed, Thin-Walled Beams", Introduction to Aircraft Structural Analysis, 2010. Publication	1%
4	mafiadoc.com Internet Source	1%
5	Submitted to University of Illinois at Urbana-Champaign Student Paper	1%
6	docero.net Internet Source	1%
7	Ted L. Lomax. "Structural Loads Analysis for Commercial Transport Aircraft", American Institute of Aeronautics and Astronautics (AIAA), 1996 Publication	1%

8	Submitted to Cranfield University Student Paper	1%
9	Submitted to University of Glamorgan Student Paper	<1%
10	Submitted to Kingston University Student Paper	<1%
11	ntnuopen.ntnu.no Internet Source	<1%
12	Submitted to University of Sheffield Student Paper	<1%
13	Egbert Torenbeek. "Advanced Aircraft Design", Wiley, 2013 Publication	<1%
14	Mario Asselin. "Operational Aircraft Performance and Flight Test Practices", American Institute of Aeronautics and Astronautics (AIAA), 2021 Publication	<1%
15	Trevor M. Young. "Performance of the Jet Transport Airplane: Analysis Methods, Flight Operations and Regulations", Wiley, 2017 Publication	<1%
16	Submitted to University of New South Wales Student Paper	<1%

17	Submitted to Michigan Technological University Student Paper	<1%
18	Submitted to Universiti Teknologi MARA Student Paper	<1%
19	Submitted to Imperial College of Science, Technology and Medicine Student Paper	<1%
20	Submitted to University of Canterbury Student Paper	<1%
21	jesuviraj.blogspot.com Internet Source	<1%
22	cgspace.cgiar.org Internet Source	<1%
23	Submitted to Emirates Aviation College, Aerospace & Academic Studies Student Paper	<1%
24	elodieroux.com Internet Source	<1%
25	www.yamawa.eu Internet Source	<1%
26	Submitted to Coventry University Student Paper	<1%
27	Mohammad Sadraey. "A Systematic Approach in Aircraft Configuration Design Optimization",	<1%

The 26th Congress of ICAS and 8th AIAA ATIO, 2008
Publication

28	Submitted to University of Hertfordshire Student Paper	<1 %
29	digitalcommons.usu.edu Internet Source	<1 %
30	Submitted to University College London Student Paper	<1 %
31	core.ac.uk Internet Source	<1 %
32	www.slideshare.net Internet Source	<1 %
33	1library.net Internet Source	<1 %
34	T.H.G. Megson. "Bending of open and closed, thin-walled beams", Elsevier BV, 2017 Publication	<1 %
35	R. Capata, L. Marino, E. Sciubba. "A hybrid propulsion system for a high-endurance UAV: configuration selection, aerodynamic study, and gas turbine bench tests", Journal of Unmanned Vehicle Systems, 2014 Publication	<1 %
36	www.govinfo.gov Internet Source	<1 %

37	Cameron Langley, Rachel Burt, Nirali Patel, Isais Martinez, Armando Leon, Timothy T. Takahashi. "Conceptual Design of a Mach 0.95 Cruise N+1 Commercial Transport", 53rd AIAA Aerospace Sciences Meeting, 2015 Publication	<1 %
38	S. Jagannathan. "Monohull research vessel seakeeping and criteria", OCEANS 88 A Partnership of Marine Interests Proceedings, 1988 Publication	<1 %
39	Trevor M. Young. "Maneuver Performance of Fixed-Wing Transport Aircraft", Wiley, 2010 Publication	<1 %
40	etd.aau.edu.et Internet Source	<1 %
41	rahauav.com Internet Source	<1 %
42	soar.wichita.edu Internet Source	<1 %
43	www.researchgate.net Internet Source	<1 %
44	Jin Guang Teng. "Buckling of Thin Shells: Recent Advances and Trends", Applied Mechanics Reviews, 1996 Publication	<1 %

Curriculum Vitae

	Basic Information
Name	Kinesha Rahma Kinanti
Place of Birth	Tangerang, Indonesia
Date of Birth	February 24, 2001
Address	Cengkareng, Jakarta Barat, DKI Jakarta, Indonesia
Year	**Education**
2019 - present	International University Liaison Indonesia
2016 - 2019	SMAN 84 Jakarta (Senior High School)
2013 - 2016	SMPI Al-Azhar 10 Kembangan (Junior High School)
2007 - 2013	SDN 09 Duri Kosambi (Elementary School)
Year	**Courses**
2020	Basic Maintenance Training - UNSURYA
Year	**Seminars & Workshops**
2021	AIAA Composite Material Seminar
2020	Basic Maintenance Training Workshop - UNSURYA
Year	**Organization Experiences**
2021	Chair of HIMA AVE IULI
2020	Member of HIMA AVE IULI
2017	Head of Training and Development Division of Karya Ilmiah Remaja
2015	Head of Decoration Commitee of "Revortal" Art Exhibition
2015	Head of Decoration Commitee of Al-Azhar Gala Dinner
2015	Head Editor of Colarixa Year Book